

Full-spectrum cone sensitivity functions for X-chromosome-linked anomalous trichromats

Paul DeMarco,* Joel Pokorny, and Vivianne C. Smith

Visual Sciences Center, The University of Chicago, 939 East 57th Street, Chicago, Illinois 60637

Received December 23, 1991; revised manuscript received March 20, 1992; accepted March 23, 1992

We derived the cone fundamentals for X-chromosome-linked anomalous trichromats for the wavelength range of 400–700 nm. Pigment templates were constructed from the cone fundamentals of normal trichromats after correction for ocular media absorption. The resultant retinal-level sensitivities had small irregularities in the short-wavelength region that were smoothed. The pigment templates, expressed as quantal sensitivities, were then shifted on a frequency abscissa to solve for the λ_{\max} of the pigments of anomalous trichromats needed to predict average anomaloscope matching data. We found that the protanomalous M- and L-cone pigments are separated by 10 nm and the deuteranomalous M'- and L-cone pigments are separated by 6 nm (rounded to the nearest nanometer), where M and L indicate middle- and long-wavelength sensitive, respectively. The triads of peak wavelengths for the corneal energy-based sensitivities were as follows: normal: 440, 543, and 566 nm; protanomalous: 440, 543, and 553 nm; and deuteranomalous: 440, 560, and 566 nm.

INTRODUCTION

For observers with normal color vision, estimates of cone spectral sensitivities are routinely used to provide the information concerning the initial transformation from physical energy to neural signals.^{1–3} Such estimates are also required for calibration of color stimulus displays for cone excitation when these displays generate stimuli by using mixtures of primary lights, such as color video displays. To calculate cone excitation for color displays and other broadband chromatic stimuli, it is necessary to have the spectral sensitivities for the cone types of each class of observer over the visible spectrum. Smith and Pokorny¹ described a set of cone fundamentals for normal observers, and here we provide a parallel set of fundamentals for X-chromosome-linked anomalous trichromats.

X-chromosome-linked anomalous trichromacy is relatively common in the United States. Approximately 5% of U.S. males have deuteranomalous trichromacy, and a further 1% have protanomalous trichromacy. Anomalous trichromats are considered to have an altered form of normal color vision.⁴ They require three primaries to match any spectral color but do not accept the color matches of color-normal trichromats. Thus it is assumed that they have three cone types with three different photopigments. This is opposed to the situation for dichromats, who are described as having a reduced form of color vision. Only two cone types having two different photopigments are revealed when dichromats are tested with a 2° foveal field.^{5–7}

Recent advances in molecular genetics have led to the cloning and the sequencing of the human X-chromosomal cone photopigments.⁸ In color-normal observers, there are one to five genes in tandem array. According to the hypothesis of Nathans *et al.*, which was based on an analysis of restriction fragment polymorphism in normal and color-defective observers,⁹ the first gene in the array encodes the opsin of the long-wavelength-sensitive (L-cone) photopigment, and the remaining genes encode opsins of

the middle-wavelength-sensitive (M-cone) photopigment. Anomalous trichromats showed major abnormalities in the gene array, with deletions of the normal genes and the presence of fusion genes (genes combining fragments of the L-cone opsin gene and fragments of the M-cone opsin gene). The deuteranomalous trichromats had a normal L-cone opsin gene, one or more fusion genes, and usually one or more M-cone opsin genes. The protanomalous trichromats had a fusion gene and one or more M-cone opsin genes.

The genetic findings in anomalous trichromats are most consistent with the prevalent model of anomalous trichromacy based on psychophysics. This model, the single-pigment-shift model, proposes that anomalous trichromats have only one pigment that differs from those of normals: the M-cone pigment for deuteranomalous trichromats or the L-cone pigment for protanomalous trichromats.^{6,10} Both types of anomalous trichromat are presumed to have the normal short-wavelength-sensitive (S-cone) pigment. For example, deuteranomalous trichromats have normal S-cone and L-cone pigments, but the λ_{\max} of the M-cone pigment, here designated M', is shifted to a longer wavelength relative to that of the normal pigment. For protanomalous trichromats, the S-cone and the M-cone pigments are normal but the λ_{\max} of the L-cone pigment, here designated L', is shifted to a shorter wavelength relative to that of the normal pigment.

The single-pigment-shift model has been used^{11,12} in conjunction with Vos–Walraven fundamentals¹³ and Schmidt's¹⁴ anomaloscope matching data to solve the λ_{\max} for the anomalous pigments required for prediction of the anomalous quotients for protanomalous and deuteranomalous trichromats. This exercise involved a number of assumptions. First it was assumed that König fundamentals^{15,16} were representative of average normal observers and, similarly, that the Schmidt anomaloscope data were representative of average anomalous trichromats. Factors such as the ocular media and the optical density of

the photopigments were assumed to be identical in such average observers. There was a further assumption that the photopigment spectra, expressed as quantal sensitivities at a retinal level, remained shape invariant for small shifts on the frequency axis. The λ_{\max} of the deuteranomalous M' pigment was found to be shifted to longer wavelengths than that of the normal M-cone pigment; the λ_{\max} of the protanomalous L' pigment was found to be shifted to shorter wavelengths than that of the normal L-cone pigment. Pokorny *et al.*¹¹ plotted and tabulated spectral sensitivity curves for the anomalous pigments between 500 and 700 nm. The short-wavelength region of the spectrum was avoided for two reasons: First, there was considerable uncertainty about both the spectral shape and the peak density of the lens and the macular pigment needed to correct for the ocular media at short wavelengths. Second there were no good estimates of the absorptivity of the human cone photopigments at that time, especially for the short-wavelength region. Then, the best estimate of the shape of the absorption spectra for M and L cones was that derived by Wald *et al.*¹⁷ for chicken iodopsin. Today, however, full-spectrum absorptivity curves of normal primate cone photopigments are available,^{18,19} permitting a comparison of psychophysical fundamentals with photopigment spectra over a full wavelength range. In the present study we combine the cur-

rent knowledge regarding the shape of photopigment spectra with psychophysical data to derive cone fundamentals for anomalous trichromats that span the wavelength range 400–700 nm.

METHODS AND RESULTS

The basic procedure followed that outlined previously^{11,12} and involved a similar set of assumptions. In the following paragraphs, we list these assumptions.

- Both normal and anomalous observers can be characterized by average photopigments. The Smith–Pokorny fundamentals¹ provide an estimate of the normal L- and M-cone sensitivities at the cornea for an observer whose color matches are those of the Judd observer.²⁰ The assumption implies only minor interobserver variation in photopigment spectra. Studies of primate photopigments support the concept of only minor variation in absorption spectra, both within and between retinas.¹⁸ However, studies of human cone photopigments, including microspectrophotometry,²¹ Rayleigh matching,²² and the most recent molecular work,^{23,24} have suggested a polymorphism of the L-cone pigment in the U.S. population with two types of L-cone photopigment separated by ~5 nm. The König L fundamental might thus represent an average of the

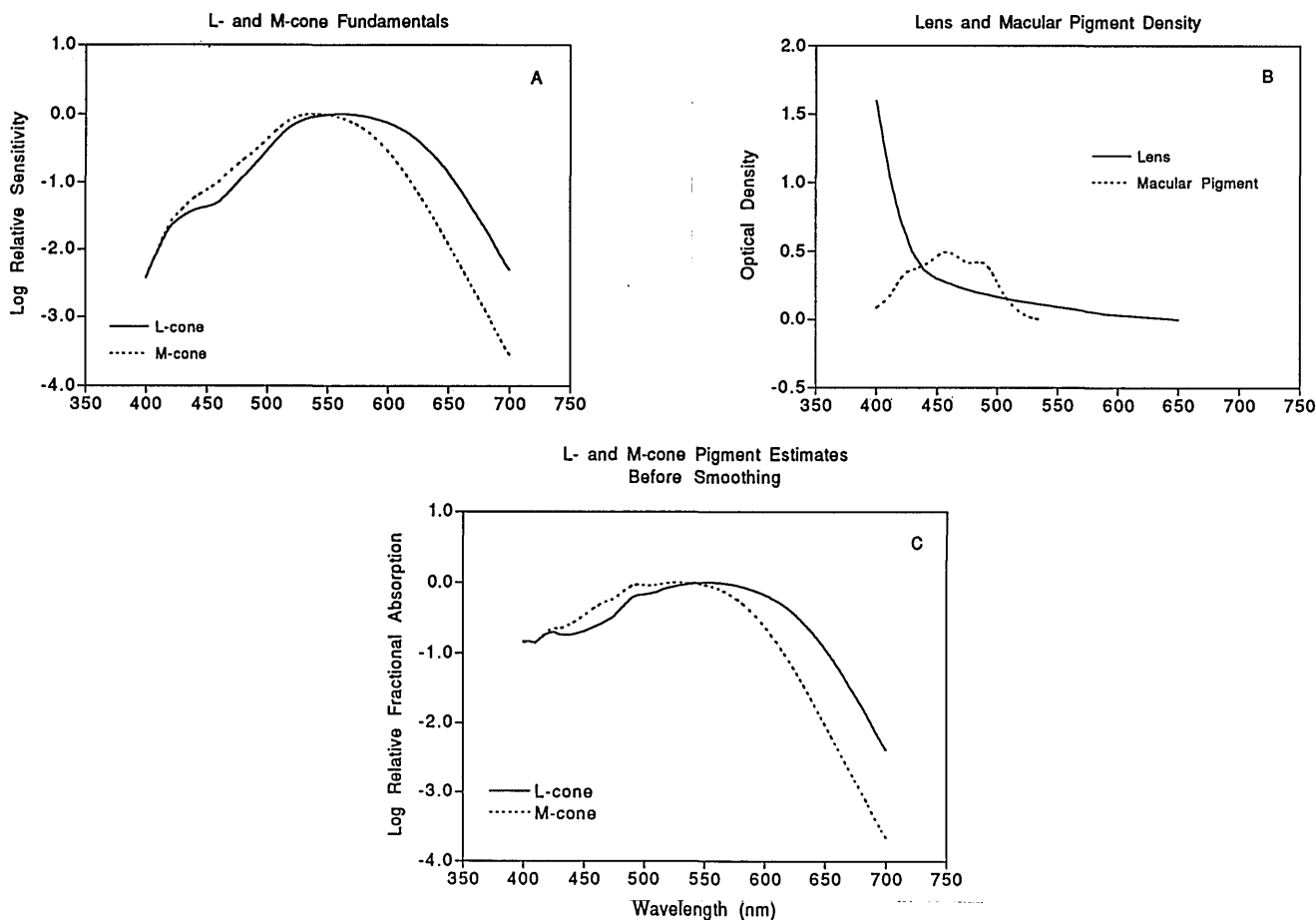


Fig. 1. A, Smith–Pokorny¹ M- and L-cone fundamentals plotted at 1-nm intervals, converted to a quantal-energy basis. B, Light absorption by the macular pigment and lens.^{32,33} C, Effects of subtracting absorption by ocular media from plot A. This gives preliminary estimates of the fractional absorption for M- and L-cone photopigments for a 2° foveal field. Note the irregularities that appear below 550 nm on both functions.

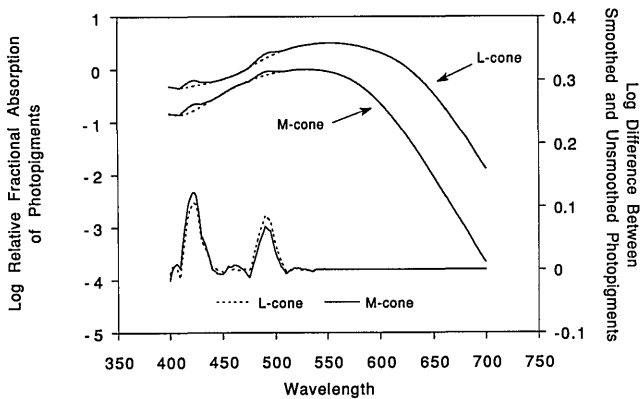


Fig. 2. Top: M- and L-cone photopigments of Fig. 1C before (smooth curves) and after (dotted curves under humps) the addition of polynomials fitted through irregular areas at shorter wavelengths. Bottom: Log difference between the smoothed and the unsmoothed regions of the photopigment estimates.

these photopigments. This would violate our assumption. The practical effect, however, would be to cause an inaccuracy in our estimate of the L- and the L-cone spectral peaks of 2–3 nm.

The concept of average photopigments in anomalous trichromats is supported by Schmidt's¹⁴ psychophysical data. Schmidt reported data from a large population of normal and simple anomalous trichromats and found that the red/green-mixture data fell into three discrete distributions. Schmidt reported the mean anomalous quotients (the ratio of green to red light for a given observer divided by the normal mean ratio of green to red light) for these distributions. The mean anomalous quotients were 1.00 for normals, 0.25 for protanomalous observers, and 3.55 for deuteranomalous observers. The distributions of the anomalous quotients for each group of observers were similar in shape, suggesting a common source of variability within the groups.

2. Normal and anomalous trichromats share similar ocular media and optical densities of cone pigments. The Schmidt¹⁴ data were gathered on 17–23-year-old military recruits. Thus the assumption of similar lens densities for the average color-normal observer, the average deuteranomalous observer, and the average protanomalous observer seems reasonable. The macular pigment should not play a role in Rayleigh matches. The hypothesis that the optical densities of photopigments of normal and anomalous trichromats are similar is supported by studies that show parallel shifts in Rayleigh matches under conditions in which photopigment density is low.²⁵

3. We assume that cone photopigment spectra are relatively shape invariant when plotted as a function of frequency, especially for small shifts along the frequency axis.^{26,27} Other abscissa transformations have been proposed by Barlow²⁸ and Mansfield²⁹ and may be useful for providing a wider range of shifts in λ_{\max} . From Pokorny *et al.*¹¹ we expected shifts of less than 10 nm to predict the behavior of anomalous trichromats. Any advantage offered by the Barlow²⁸ or the Mansfield²⁹ technique would, in our case, be negligible. We used the following conservative approach to estimate pigment shapes: The expected differences in λ_{\max} between the anomalous pigment and the normal pigment are ~ 7 nm. We used the tem-

plate for the normal M-cone pigment to estimate the shape of the protanomalous L-cone pigment. Likewise, we used the template for the normal L-cone pigment to estimate the shape of the deuteranomalous M'-cone pigment.

We start by taking the Smith-Pokorny¹ M- and L-cone fundamentals, derived from the Judd-Vos observer^{20,30} interpolated to 1-nm intervals, and converting them from an equal-energy spectrum to a quantal-energy spectrum. This transformation is performed by dividing the sensitivity values at each wavelength λ by the ratio $\lambda/700$. The results are shown in Fig. 1A. Because we assume that the optical density of the average anomalous trichromat is similar to that of the average normal trichromat, all the calculations were performed with the fundamentals expressed in units of fractional absorption rather than absorptivity.³¹ This procedure obviates the assumption of an explicit value for effective optical density in the 2° colorimetric field.

To correct for absorption by the lens and the macular pigment, we used the lens absorption data from Pokorny

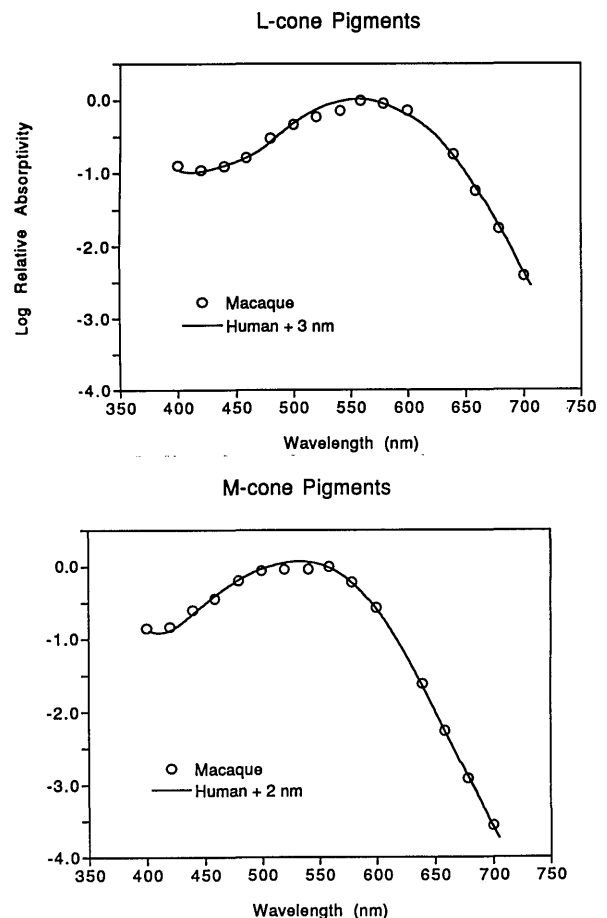


Fig. 3. Comparison of the smoothed human M- and L-cone photopigment estimates in absorptivity with the spectral sensitivity measurements from isolated M and L cones of the macaque retina.¹⁸ The macaque data are mean spectral sensitivities for approximately 20 M and 16 L cones. The human pigment templates required a shift in λ_{\max} to fit the monkey data and are plotted. The M-cone pigment template was shifted +2 nm, and the L-cone template was shifted +3 nm. The spectra were shifted on a frequency abscissa and then replotted on a wavelength abscissa for comparisons.

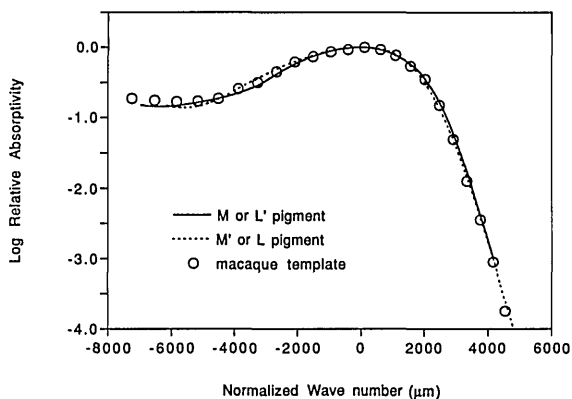


Fig. 4. Comparison of the cone photopigment template proposed by Baylor *et al.*,¹⁸ gathered from recordings from single macaque L and M cones and rods, and the derived L' and M' photopigments in absorptivity. Note that all the pigment spectra are smooth functions in the middle- to short-wavelength regions of the spectrum.

*et al.*³² for a 32-year-old observer with a small entrance pupil. We used the macular pigment absorption data from Wyszecki and Stiles.³³ Both of these curves are

shown in Fig. 1B. After subtracting the effects of the ocular media (Fig. 1C), we obtain estimates of the fractional absorption of the M- and the L-cone photopigments at a retinal level. These estimates show irregularities in the short-wavelength region of the spectrum. Breton and Massof³⁴ also reported such irregularities in the cone fundamentals when the effects of macular pigment are taken into account.

To remove the irregularities from the estimated pigment curves, we smoothed the pigment shape at the points of irregularity by using piecemeal fits of second- and third-order polynomials across the irregular regions of each curve. All the polynomial fits were scrutinized for accuracy and had chi-square values between 10^{-3} and 10^{-8} (Mathview Professional software, BrainPower Inc., Calabasas, Calif.). Shown in the upper half of Fig. 2 are plots of the M- and the L-cone photopigments with the polynomial bridges plotted as dotted curves over the irregular regions. The sensitivity difference between the smoothed curves and the raw data was recorded, and the irregular portions of the curves were then removed so that the pigments were smooth throughout these regions. The difference between the pigments before and after smoothing is shown near the bottom of Fig. 2, along with a plot of the

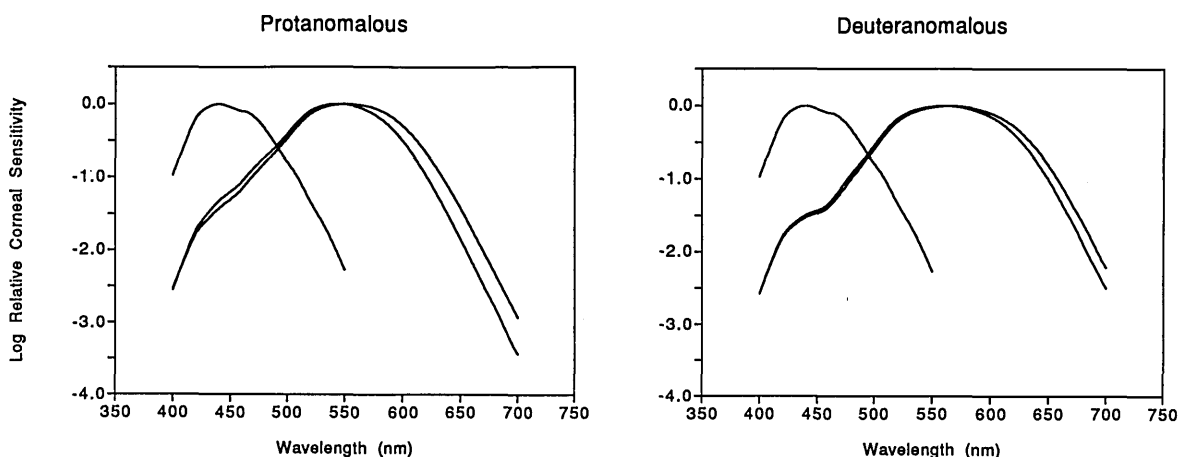


Fig. 5. Estimates of the cone fundamentals for deuteranomalous and protanomalous trichromats plotted at 1-nm intervals.

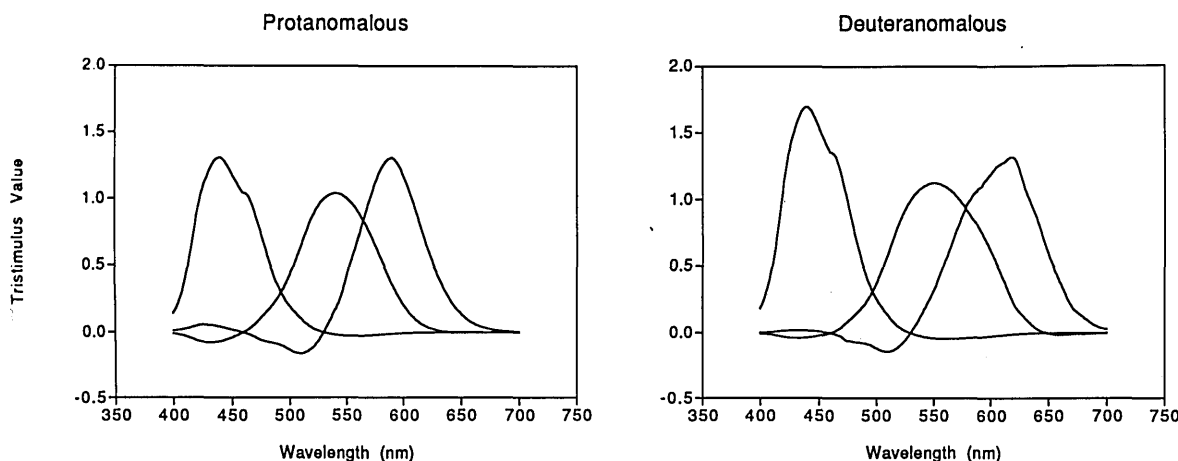


Fig. 6. Theoretical color-matching functions for deuteranomalous and protanomalous trichromats. They were calculated from the cone fundamentals of Fig. 5, using the method of Wright⁴¹ for an equal-energy spectrum and primaries at 450, 530, and 650 nm.

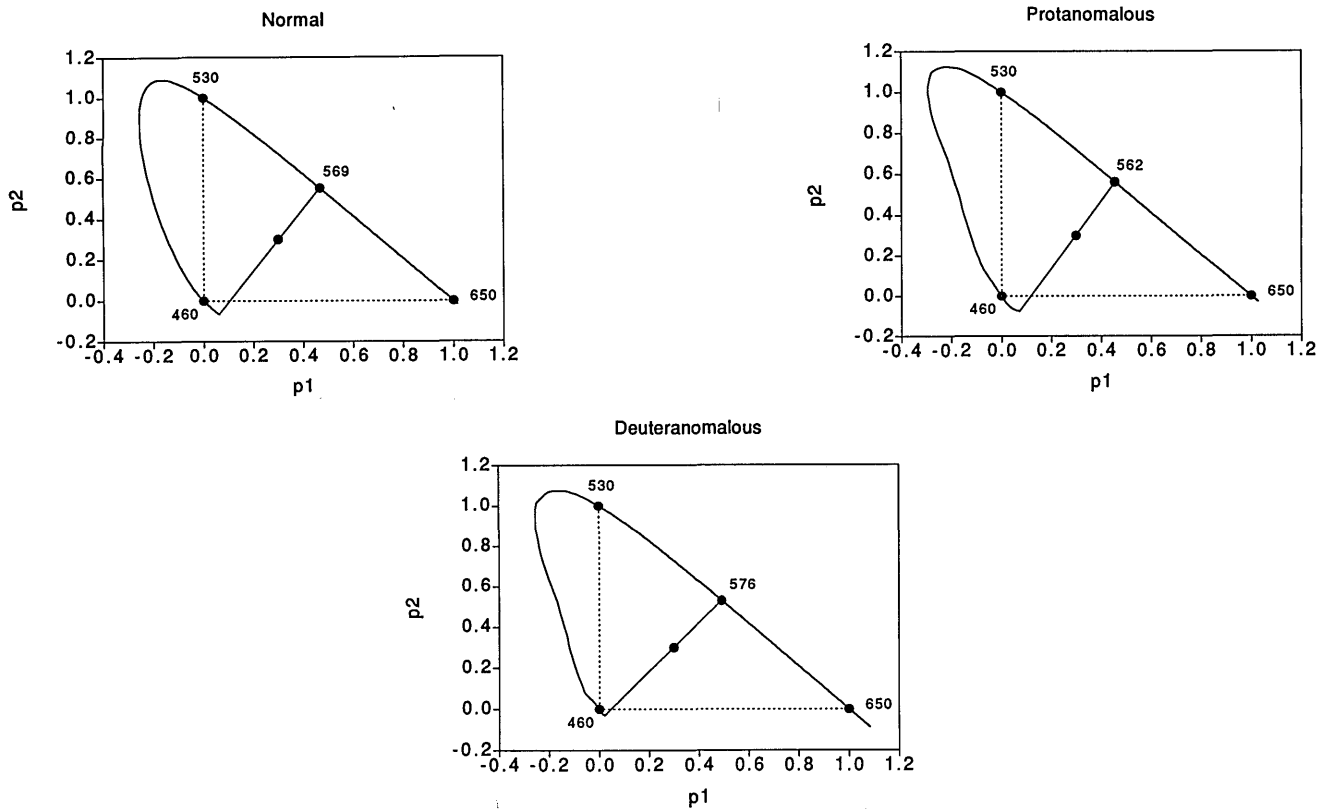


Fig. 7. Chromaticity diagrams constructed from the color-matching functions and primaries of Fig. 6, along with the diagram for normal trichromats, using the Smith-Pokorny¹ fundamentals. The dotted lines define the major axes of the plots, which run through the points where the three color-matching primaries would lie. The filled circle near the center of each diagram is the point of equal-energy white. The line running through white connects the calculated achromatic point for each type of trichromat and the blue corner of the diagram.

pigments before smoothing. The independent smoothing performed for each pigment reveals a common source of irregularity for both pigments.

The irregularities characterized in Fig. 2 may represent additional ocular media error, either lens data or more likely the macular pigment absorption, or may be a consequence of the minor smoothing of the original Wright³⁵ and Guild³⁶ colorimetric data when the CIE Standard Observer was created.³⁷ In fact, because preretinal absorption certainly must affect psychophysical spectral sensitivity, one expects to see irregularities of preretinal absorption in psychophysical cone fundamentals and the color-matching functions from which the fundamentals are derived. Considerations such as data smoothing, coarse wavelength steps, and interobserver variability may contribute to the absence of such irregularities from standardized response functions.

At this point it is instructive to compare our pigment estimates with spectral sensitivity data obtained from single primate photoreceptors. Baylor *et al.*¹⁸ obtained such spectral sensitivity measurements by recording the photocurrent of individual cones from the macaque retina. Figure 3 shows their averaged data from 20 M cones and 16 L cones. Also shown are our estimates of the human M- and L-cone photopigments, now corrected for self-screening by the assumption of optical densities of 0.3 and 0.4 for the M-cone and the L-cone pigments, respectively.³⁸

We found that, to fit the macaque data, a minor shift in λ_{\max} of the human pigments to longer wavelengths was necessary (shifts were performed on a frequency abscissa). We shifted the human M-cone pigment template +2 nm and the L-cone template +3 nm to obtain a good congruence with the macaque data. Because of the variability in the macaque data, coupled with a relatively small data set from human retinas by this technique,³⁹ we cannot be sure whether this wavelength shift represents a true interspecies difference⁴⁰ or a methodological difference. However, without this shift the data sets were considerably displaced across the entire spectrum, not just at the peak. Baylor *et al.*¹⁸ also published a polynomial template derived from the data set of cone spectral sensitivities that were normalized on a log frequency abscissa. We compared the shape of the macaque cone template with the shape of our human pigment estimates and found an excellent correspondence. Figure 4 shows this comparison by plotting the curves on a normalized frequency scale. The degree of correspondence suggests that our smoothing procedures yield good estimates of the spectral sensitivity curves of human cone pigments and correctly discount the effects of absorption by the lens and the macular pigment.

In preparation to solve the anomalous Rayleigh equations, we replotted the pigments on a frequency abscissa and fitted a third- or a fourth-order polynomial to the regions of each pigment template that encompassed the test

and the primary wavelengths used in the Rayleigh match. These polynomials allowed us to step in small increments to solve precisely the Rayleigh equation for the anomalous quotients. To solve for the anomalous quotient of deuteranomalous trichromats, the template for the L-cone pigment was duplicated and shifted against a fixed template for the L-cone pigment until a set of simultaneous Rayleigh match equations was solved to produce an anomalous quotient of 3.55 for deuteranomalous trichromats. To solve for the anomalous quotient of protanomalous trichromats, the template for the M-cone pigment was duplicated and shifted against a fixed template for the M-cone pigment to solve for an anomalous quotient of 0.25.

The procedure gave us estimates of the protanomalous L'-cone photopigment and the deuteranomalous M'-cone photopigment. We found that the protanomalous M- and L'-cone pigments are separated by 10 nm and the deuteranomalous M'- and L-cone pigments are separated by 6 nm (rounded to the nearest nanometer). These estimates are in reasonable agreement with the previous estimates^{11,12} of an 8–9-nm difference in λ_{\max} between the protanomalous pigments and a 5–6-nm difference in λ_{\max} between the deuteranomalous pigments. The small differences presumably reflect minor variations in the fitting procedures among the three studies. The separation of the M'- and the L'-cone pigments for deuteranomalous trichromats is similar to that postulated to occur as a natural polymorphism of the L-cone pigment in color-normal males.^{23,24}

We then reconstructed cone fundamentals from the photopigments by adding back filtering from the lens and the macular pigments and the irregularities previously removed by the smoothing operation. Figure 5 shows the resultant curves as a function of wavelength for an equal-energy spectrum, together with the normal S-cone fundamental normalized to its peak. For these cone fundamentals, the λ_{\max} of the L' fundamental for protanomalous trichromats is at 553 nm, and the λ_{\max} of the M' fundamental for deuteranomalous trichromats is at 560 nm. Appendix A provides the relative sensitivity values of the S-, M-, L-, M'-, and L'-cone fundamentals at 1-nm intervals.

Using the estimates of the anomalous cone fundamentals, we derived theoretical color-matching functions and chromaticity diagrams for anomalous trichromats. Figure 6 shows the theoretical color-matching functions for deuteranomalous and protanomalous trichromats computed by using Wright's⁴¹ primary system, the primaries of 450, 530, and 650 nm. These color-matching functions were normalized to an equal-energy white so that each curve has an equal area under it.

The color-matching functions were constructed by solving three simultaneous linear equations at each wavelength (1-nm intervals) that expressed a color match for a

given wavelength as a sum of the sensitivities of the three cone fundamentals. Figure 7 shows chromaticity diagrams for the normal and the two types of anomalous trichromat. The dotted lines show the major axes of the plot that run through the primaries.

With normalization to white, the expected null coordinate of a first-stage spectral opponent can be calculated. This corresponds to the tritan neutral point in color-normal individuals and the wavelength of minimum colorimetric purity. According to Thornton and Pugh,⁴² this point is also associated with the percept of a color containing neither redness or greenness. We calculated the null coordinates for protanomalous and deuteranomalous trichromats and found them to occur at 562 and 576 nm, respectively. A line connecting the null point, white, and extending to the blue corner is shown for each type of trichromat. These wavelength shifts along the red/green axis of the chromaticity diagrams are consistent with shifts in unique yellow for deuteranomalous and protanomalous observers relative to the locus of unique yellow of normals.^{10,43}

COMMENT

The full-spectrum cone fundamentals that we derived should be useful for modeling the spectral response cone of anomalous trichromats in psychophysical experiments. The fundamentals should also be useful in studies in which the experimenter wishes to account for the expected color performance of simple anomalous trichromats, for example, to calibrate a color monitor. Such a calibration would be necessary to compensate for differences in metameric matches between color-normal and anomalous trichromatic observers, permitting the precise specification of the stimulus despite the reduced discrimination ability of anomalous trichromats. The calibration is also necessary for the computation of equivalent steps in chromaticity for normal and anomalous observers. One could also predict shifts in the perception of hue under conditions in which anomalous trichromats are exposed to colored papers or broadband spectral lights, using the color-matching functions to produce a chromaticity diagram for the appropriate anomaly.⁴⁴

ACKNOWLEDGMENTS

This research was supported in part by National Eye Institute grants R01-EY00901 (J. Pokorny) and F32-EY6252 (P. DeMarco).

*Present address, Department of Neurology, Loyola University Medical Center, 2160 South First Avenue, Maywood, Illinois 60153.

Requests for reprints should be addressed to J. Pokorny.

Appendix A. Relative Sensitivity Values (in Linear Units) for Normal and Anomalous Cone Fundamentals and the Associated Pigment Estimates in Absorptivity for the M and the L Cones (All Functions Normalized to Peak Sensitivity)

Wavelength	Psychophysical Cone Fundamentals					Pigment Extinction Spectra				Lens	Macular
	S	M	L	M'	L'	L	M	L'	M'	Density	Density
400	1.0768E-1	2.8229E-3	2.6555E-3	2.6556E-3	2.9518E-3	1.0410E-1	1.1099E-1	1.2234E-1	1.0092E-1	1.600E+0	8.50E-2
401	1.1994E-1	3.1464E-3	2.9520E-3	2.9661E-3	3.2651E-3	1.0293E-1	1.0949E-1	1.1994E-1	1.0023E-1	1.549E+0	9.20E-2
402	1.3318E-1	3.4982E-3	3.2716E-3	3.3017E-3	3.6028E-3	1.0192E-1	1.0816E-1	1.1770E-1	9.9689E-2	1.499E+0	9.90E-2
403	1.4746E-1	3.8809E-3	3.6155E-3	3.6638E-3	3.9669E-3	1.0106E-1	1.0701E-1	1.1564E-1	9.9276E-2	1.448E+0	1.06E-1
404	1.6285E-1	4.2967E-3	3.9850E-3	4.0542E-3	4.3588E-3	1.0036E-1	1.0605E-1	1.1374E-1	9.8988E-2	1.397E+0	1.13E-1
405	1.7946E-1	4.7486E-3	4.3826E-3	4.4753E-3	4.7802E-3	9.9787E-2	1.0526E-1	1.1202E-1	9.8818E-2	1.347E+0	1.20E-1
406	1.9732E-1	5.2398E-3	4.8103E-3	4.9296E-3	5.2326E-3	9.9348E-2	1.0467E-1	1.1046E-1	9.8758E-2	1.296E+0	1.28E-1
407	2.1658E-1	5.7741E-3	5.2710E-3	5.4202E-3	5.7190E-3	9.9032E-2	1.0425E-1	1.0907E-1	9.8802E-2	1.245E+0	1.36E-1
408	2.3743E-1	6.3545E-3	5.7683E-3	5.9513E-3	6.2408E-3	9.8831E-2	1.0403E-1	1.0786E-1	9.8943E-2	1.194E+0	1.44E-1
409	2.6012E-1	6.9850E-3	6.3064E-3	6.5272E-3	6.7999E-3	9.8740E-2	1.0400E-1	1.0681E-1	9.9174E-2	1.144E+0	1.52E-1
410	2.8485E-1	7.6700E-3	6.8892E-3	7.1524E-3	7.3987E-3	9.8751E-2	1.0415E-1	1.0594E-1	9.9491E-2	1.093E+0	1.60E-1
411	3.1368E-1	8.4687E-3	7.5667E-3	7.8754E-3	8.0894E-3	9.8857E-2	1.0451E-1	1.0524E-1	9.9887E-2	1.057E+0	1.73E-1
412	3.4491E-1	9.3426E-3	8.3002E-3	8.6575E-3	8.8420E-3	9.9054E-2	1.0505E-1	1.0471E-1	1.0036E-1	1.021E+0	1.86E-1
413	3.7854E-1	1.0294E-2	9.0902E-3	9.4992E-3	9.6576E-3	9.9335E-2	1.0579E-1	1.0436E-1	1.0090E-1	9.850E-1	1.99E-1
414	4.1447E-1	1.1322E-2	9.9350E-3	1.0399E-2	1.0535E-2	9.9696E-2	1.0672E-1	1.0419E-1	1.0150E-1	9.490E-1	2.12E-1
415	4.5258E-1	1.2424E-2	1.0833E-2	1.1355E-2	1.1471E-2	1.0013E-1	1.0786E-1	1.0420E-1	1.0217E-1	9.130E-1	2.25E-1
416	4.9264E-1	1.3596E-2	1.1780E-2	1.2362E-2	1.2460E-2	1.0063E-1	1.0919E-1	1.0440E-1	1.0289E-1	8.770E-1	2.40E-1
417	5.3407E-1	1.4834E-2	1.2766E-2	1.3411E-2	1.3500E-2	1.0120E-1	1.1072E-1	1.0477E-1	1.0367E-1	8.410E-1	2.55E-1
418	5.7611E-1	1.6135E-2	1.3777E-2	1.4488E-2	1.4586E-2	1.0183E-1	1.1244E-1	1.0533E-1	1.0449E-1	8.050E-1	2.70E-1
419	6.1812E-1	1.7495E-2	1.4802E-2	1.5580E-2	1.5712E-2	1.0251E-1	1.1437E-1	1.0608E-1	1.0536E-1	7.690E-1	2.85E-1
420	6.5924E-1	1.8901E-2	1.5822E-2	1.6670E-2	1.6865E-2	1.0325E-1	1.1650E-1	1.0701E-1	1.0628E-1	7.330E-1	3.00E-1
421	6.9444E-1	2.0205E-2	1.6717E-2	1.7626E-2	1.7921E-2	1.0404E-1	1.1883E-1	1.0812E-1	1.0724E-1	7.090E-1	3.09E-1
422	7.2764E-1	2.1510E-2	1.7581E-2	1.8553E-2	1.8964E-2	1.0487E-1	1.2136E-1	1.0942E-1	1.0823E-1	6.850E-1	3.18E-1
423	7.5860E-1	2.2807E-2	1.8412E-2	1.9445E-2	1.9985E-2	1.0575E-1	1.2409E-1	1.1091E-1	1.0926E-1	6.610E-1	3.27E-1
424	7.8713E-1	2.4092E-2	1.9207E-2	2.0303E-2	2.0982E-2	1.0667E-1	1.2702E-1	1.1259E-1	1.1033E-1	6.370E-1	3.36E-1
425	8.1312E-1	2.5365E-2	1.9967E-2	2.1126E-2	2.1952E-2	1.0763E-1	1.3015E-1	1.1447E-1	1.1143E-1	6.130E-1	3.45E-1
426	8.3652E-1	2.6628E-2	2.0693E-2	2.1921E-2	2.2868E-2	1.0862E-1	1.3349E-1	1.1653E-1	1.1257E-1	5.890E-1	3.49E-1
427	8.5751E-1	2.7886E-2	2.1387E-2	2.2687E-2	2.3754E-2	1.0965E-1	1.3702E-1	1.1877E-1	1.1374E-1	5.650E-1	3.53E-1
428	8.7621E-1	2.9145E-2	2.2052E-2	2.3427E-2	2.4617E-2	1.1071E-1	1.4076E-1	1.2120E-1	1.1494E-1	5.410E-1	3.57E-1
429	8.9283E-1	3.0416E-2	2.2693E-2	2.4144E-2	2.5465E-2	1.1181E-1	1.4469E-1	1.2383E-1	1.1617E-1	5.170E-1	3.61E-1
430	9.0754E-1	3.1709E-2	2.3314E-2	2.4846E-2	2.6305E-2	1.1294E-1	1.4883E-1	1.2665E-1	1.1744E-1	4.930E-1	3.65E-1
431	9.2474E-1	3.3185E-2	2.4029E-2	2.5630E-2	2.7382E-2	1.1409E-1	1.5317E-1	1.2966E-1	1.1873E-1	4.797E-1	3.68E-1
432	9.4039E-1	3.4705E-2	2.4737E-2	2.6409E-2	2.8488E-2	1.1528E-1	1.5771E-1	1.3286E-1	1.2007E-1	4.664E-1	3.71E-1
433	9.5439E-1	3.6262E-2	2.5440E-2	2.7185E-2	2.9613E-2	1.1650E-1	1.6244E-1	1.3624E-1	1.2143E-1	4.531E-1	3.74E-1
434	9.6666E-1	3.7850E-2	2.6138E-2	2.7959E-2	3.0753E-2	1.1776E-1	1.6738E-1	1.3982E-1	1.2283E-1	4.398E-1	3.77E-1
435	9.7713E-1	3.9462E-2	2.6833E-2	2.8732E-2	3.1900E-2	1.1904E-1	1.7251E-1	1.4358E-1	1.2428E-1	4.265E-1	3.80E-1
436	9.8551E-1	4.1089E-2	2.7519E-2	2.9499E-2	3.3059E-2	1.2036E-1	1.7784E-1	1.4754E-1	1.2576E-1	4.132E-1	3.84E-1
437	9.9187E-1	4.2731E-2	2.8195E-2	3.0258E-2	3.4219E-2	1.2171E-1	1.8336E-1	1.5168E-1	1.2728E-1	3.999E-1	3.88E-1
438	9.9631E-1	4.4384E-2	2.8853E-2	3.1005E-2	3.5374E-2	1.2309E-1	1.8908E-1	1.5601E-1	1.2885E-1	3.866E-1	3.92E-1
439	9.9897E-1	4.6043E-2	2.9488E-2	3.1732E-2	3.6520E-2	1.2452E-1	1.9500E-1	1.6053E-1	1.3047E-1	3.733E-1	3.96E-1
440	1.0000E+0	4.7706E-2	3.0096E-2	3.2436E-2	3.7655E-2	1.2598E-1	2.0111E-1	1.6524E-1	1.3214E-1	3.600E-1	4.00E-1
441	9.9734E-1	4.9264E-2	3.0609E-2	3.3021E-2	3.8829E-2	1.2748E-1	2.0741E-1	1.7013E-1	1.3387E-1	3.540E-1	4.05E-1
442	9.9299E-1	5.0813E-2	3.1089E-2	3.3575E-2	3.9994E-2	1.2903E-1	2.1390E-1	1.7521E-1	1.3565E-1	3.480E-1	4.10E-1
443	9.8697E-1	5.2359E-2	3.1540E-2	3.4105E-2	4.1155E-2	1.3063E-1	2.2058E-1	1.8047E-1	1.3751E-1	3.420E-1	4.15E-1
444	9.7933E-1	5.3905E-2	3.1966E-2	3.4611E-2	4.2317E-2	1.3227E-1	2.2745E-1	1.8592E-1	1.3943E-1	3.360E-1	4.20E-1
445	9.7017E-1	5.5456E-2	3.2371E-2	3.5103E-2	4.3485E-2	1.3397E-1	2.3451E-1	1.9155E-1	1.4143E-1	3.300E-1	4.25E-1
446	9.5964E-1	5.7019E-2	3.2760E-2	3.5574E-2	4.4707E-2	1.3573E-1	2.4175E-1	1.9736E-1	1.4350E-1	3.240E-1	4.32E-1
447	9.4810E-1	5.8600E-2	3.3142E-2	3.6045E-2	4.5951E-2	1.3756E-1	2.4918E-1	2.0335E-1	1.4567E-1	3.180E-1	4.39E-1
448	9.3584E-1	6.0209E-2	3.3522E-2	3.6517E-2	4.7225E-2	1.3944E-1	2.5678E-1	2.0953E-1	1.4792E-1	3.120E-1	4.46E-1
449	9.2318E-1	6.1854E-2	3.3908E-2	3.7003E-2	4.8536E-2	1.4141E-1	2.6457E-1	2.1588E-1	1.5028E-1	3.060E-1	4.53E-1
450	9.1046E-1	6.3547E-2	3.4307E-2	3.7507E-2	4.9897E-2	1.4344E-1	2.7253E-1	2.2241E-1	1.5274E-1	3.000E-1	4.60E-1
451	8.9773E-1	6.5281E-2	3.4719E-2	3.8023E-2	5.1343E-2	1.4557E-1	2.8068E-1	2.2912E-1	1.5531E-1	2.967E-1	4.66E-1
452	8.8533E-1	6.7084E-2	3.5164E-2	3.8579E-2	5.2862E-2	1.4778E-1	2.8899E-1	2.3601E-1	1.5801E-1	2.934E-1	4.72E-1
453	8.7326E-1	6.8972E-2	3.5651E-2	3.9184E-2	5.4466E-2	1.5008E-1	2.9748E-1	2.4305E-1	1.6084E-1	2.901E-1	4.78E-1
454	8.6151E-1	7.0961E-2	3.6191E-2	3.9852E-2	5.6175E-2	1.5249E-1	3.0613E-1	2.5029E-1	1.6381E-1	2.868E-1	4.84E-1
455	8.5005E-1	7.3070E-2	3.6796E-2	4.0592E-2	5.8002E-2	1.5501E-1	3.1495E-1	2.5768E-1	1.6692E-1	2.835E-1	4.90E-1
456	8.3882E-1	7.5315E-2	3.7474E-2	4.1448E-2	5.9834E-2	1.5764E-1	3.2394E-1	2.6526E-1	1.7020E-1	2.802E-1	4.91E-1
457	8.2797E-1	7.7711E-2	3.8239E-2	4.2405E-2	6.1807E-2	1.6040E-1	3.3309E-1	2.7298E-1	1.7364E-1	2.769E-1	4.92E-1
458	8.1769E-1	8.0281E-2	3.9106E-2	4.3478E-2	6.3951E-2	1.6329E-1	3.4239E-1	2.8089E-1	1.7726E-1	2.736E-1	4.93E-1
459	8.0804E-1	8.3036E-2	4.0087E-2	4.4681E-2	6.6271E-2	1.6633E-1	3.5185E-1	2.8895E-1	1.8108E-1	2.703E-1	4.94E-1

(continued overleaf)

Appendix A. Continued

Wavelength	Psychophysical Cone Fundamentals					Pigment Extinction Spectra				Lens Density	Macular Density
	S	M	L	M'	L'	L	M	L'	M'		
460	7.9913E-1	8.5998E-2	4.1195E-2	4.6028E-2	6.8790E-2	1.6951E-1	3.6146E-1	2.9717E-1	1.8510E-1	2.670E-1	4.95E-1
461	7.9810E-1	8.9985E-2	4.2823E-2	4.7978E-2	7.2100E-2	1.7286E-1	3.7123E-1	3.0556E-1	1.8933E-1	2.636E-1	4.90E-1
462	7.9549E-1	9.4046E-2	4.4521E-2	5.0023E-2	7.5470E-2	1.7637E-1	3.8113E-1	3.1409E-1	1.9379E-1	2.602E-1	4.85E-1
463	7.9095E-1	9.8189E-2	4.6308E-2	5.2182E-2	7.8912E-2	1.8007E-1	3.9118E-1	3.2279E-1	1.9850E-1	2.568E-1	4.80E-1
464	7.8409E-1	1.0242E-1	4.8204E-2	5.4478E-2	8.2432E-2	1.8396E-1	4.0137E-1	3.3163E-1	2.0346E-1	2.534E-1	4.75E-1
465	7.7451E-1	1.0675E-1	5.0228E-2	5.6933E-2	8.6036E-2	1.8805E-1	4.1168E-1	3.4062E-1	2.0869E-1	2.500E-1	4.70E-1
466	7.6180E-1	1.1117E-1	5.2393E-2	5.9562E-2	8.9724E-2	1.9236E-1	4.2213E-1	3.4976E-1	2.1422E-1	2.466E-1	4.65E-1
467	7.4628E-1	1.1570E-1	5.4706E-2	6.2373E-2	9.3503E-2	1.9690E-1	4.3271E-1	3.5904E-1	2.2005E-1	2.432E-1	4.60E-1
468	7.2853E-1	1.2035E-1	5.7179E-2	6.5382E-2	9.7392E-2	2.0168E-1	4.4340E-1	3.6846E-1	2.2620E-1	2.398E-1	4.55E-1
469	7.0923E-1	1.2514E-1	5.9825E-2	6.8603E-2	1.0141E-1	2.0672E-1	4.5421E-1	3.7801E-1	2.3269E-1	2.364E-1	4.50E-1
470	6.8910E-1	1.3009E-1	6.2656E-2	7.2052E-2	1.0558E-1	2.1203E-1	4.6513E-1	3.8770E-1	2.3955E-1	2.330E-1	4.45E-1
471	6.6856E-1	1.3522E-1	6.5679E-2	7.6174E-2	1.0985E-1	2.1763E-1	4.7616E-1	3.9752E-1	2.4831E-1	2.304E-1	4.38E-1
472	6.4755E-1	1.4051E-1	6.8899E-2	8.0627E-2	1.1428E-1	2.2354E-1	4.8729E-1	4.0746E-1	2.5772E-1	2.278E-1	4.31E-1
473	6.2607E-1	1.4597E-1	7.2318E-2	8.4892E-2	1.1886E-1	2.2976E-1	4.9851E-1	4.1753E-1	2.6595E-1	2.252E-1	4.24E-1
474	6.0411E-1	1.5160E-1	7.5940E-2	8.9372E-2	1.2359E-1	2.3633E-1	5.0983E-1	4.2772E-1	2.7445E-1	2.226E-1	4.17E-1
475	5.8169E-1	1.5739E-1	7.9771E-2	9.4060E-2	1.2847E-1	2.4326E-1	5.2122E-1	4.3802E-1	2.8324E-1	2.200E-1	4.10E-1
476	5.5893E-1	1.6338E-1	8.3826E-2	9.7779E-2	1.3393E-1	2.5374E-1	5.3270E-1	4.4842E-1	2.9229E-1	2.174E-1	4.11E-1
477	5.3606E-1	1.6954E-1	8.8099E-2	1.0257E-1	1.3957E-1	2.6166E-1	5.4424E-1	4.5894E-1	3.0160E-1	2.148E-1	4.12E-1
478	5.1316E-1	1.7586E-1	9.2557E-2	1.0754E-1	1.4536E-1	2.6987E-1	5.5585E-1	4.6956E-1	3.1117E-1	2.122E-1	4.13E-1
479	4.9035E-1	1.8228E-1	9.7166E-2	1.1265E-1	1.5128E-1	2.7834E-1	5.6752E-1	4.8027E-1	3.2099E-1	2.096E-1	4.14E-1
480	4.6772E-1	1.8879E-1	1.0189E-1	1.1787E-1	1.5728E-1	2.8707E-1	5.7923E-1	4.9107E-1	3.3104E-1	2.070E-1	4.15E-1
481	4.4537E-1	1.9537E-1	1.0672E-1	1.2316E-1	1.6339E-1	2.9607E-1	5.9099E-1	5.0197E-1	3.4133E-1	2.050E-1	4.16E-1
482	4.2344E-1	2.0207E-1	1.1168E-1	1.2859E-1	1.6963E-1	3.0531E-1	6.0279E-1	5.1294E-1	3.5184E-1	2.030E-1	4.17E-1
483	4.0206E-1	2.0896E-1	1.1685E-1	1.3420E-1	1.7607E-1	3.1479E-1	6.1461E-1	5.2399E-1	3.6257E-1	2.010E-1	4.18E-1
484	3.8140E-1	2.1610E-1	1.2226E-1	1.4006E-1	1.8276E-1	3.2450E-1	6.2645E-1	5.3510E-1	3.7350E-1	1.990E-1	4.19E-1
485	3.6158E-1	2.2358E-1	1.2799E-1	1.4623E-1	1.8978E-1	3.3445E-1	6.3829E-1	5.4629E-1	3.8464E-1	1.970E-1	4.20E-1
486	3.4273E-1	2.3141E-1	1.3406E-1	1.5284E-1	1.9700E-1	3.4461E-1	6.5015E-1	5.5753E-1	3.9597E-1	1.950E-1	4.18E-1
487	3.2482E-1	2.3962E-1	1.4048E-1	1.5980E-1	2.0460E-1	3.5499E-1	6.6199E-1	5.6882E-1	4.0749E-1	1.930E-1	4.16E-1
488	3.0783E-1	2.4827E-1	1.4727E-1	1.6713E-1	2.1262E-1	3.6557E-1	6.7381E-1	5.8016E-1	4.1918E-1	1.910E-1	4.14E-1
489	2.9170E-1	2.5739E-1	1.5443E-1	1.7483E-1	2.2111E-1	3.7635E-1	6.8561E-1	5.9153E-1	4.3103E-1	1.890E-1	4.12E-1
490	2.7638E-1	2.6703E-1	1.6199E-1	1.8294E-1	2.3011E-1	3.8732E-1	6.9738E-1	6.0294E-1	4.4305E-1	1.870E-1	4.10E-1
491	2.6185E-1	2.7724E-1	1.6998E-1	1.9177E-1	2.3923E-1	3.9847E-1	7.0909E-1	6.1437E-1	4.5522E-1	1.850E-1	4.00E-1
492	2.4814E-1	2.8805E-1	1.7842E-1	2.0107E-1	2.4891E-1	4.0980E-1	7.2075E-1	6.2582E-1	4.6753E-1	1.830E-1	3.90E-1
493	2.3520E-1	2.9943E-1	1.8729E-1	2.1083E-1	2.5915E-1	4.2129E-1	7.3234E-1	6.3727E-1	4.7997E-1	1.810E-1	3.80E-1
494	2.2300E-1	3.1138E-1	1.9660E-1	2.2104E-1	2.6994E-1	4.3295E-1	7.4385E-1	6.4873E-1	4.9254E-1	1.790E-1	3.70E-1
495	2.1151E-1	3.2389E-1	2.0635E-1	2.3171E-1	2.8126E-1	4.4475E-1	7.5528E-1	6.6018E-1	5.0522E-1	1.770E-1	3.60E-1
496	2.0069E-1	3.3691E-1	2.1651E-1	2.4312E-1	2.9265E-1	4.5670E-1	7.6660E-1	6.7162E-1	5.1801E-1	1.750E-1	3.43E-1
497	1.9050E-1	3.5051E-1	2.2714E-1	2.5503E-1	3.0458E-1	4.6879E-1	7.7780E-1	6.8303E-1	5.3089E-1	1.730E-1	3.26E-1
498	1.8094E-1	3.6484E-1	2.3833E-1	2.6756E-1	3.1718E-1	4.8100E-1	7.8889E-1	6.9440E-1	5.4385E-1	1.710E-1	3.09E-1
499	1.7197E-1	3.8004E-1	2.5020E-1	2.8081E-1	3.3061E-1	4.9332E-1	7.9983E-1	7.0574E-1	5.5689E-1	1.690E-1	2.92E-1
500	1.6357E-1	3.9624E-1	2.6285E-1	2.9488E-1	3.4499E-1	5.0576E-1	8.1063E-1	7.1702E-1	5.6998E-1	1.670E-1	2.75E-1
501	1.5575E-1	4.1356E-1	2.7636E-1	3.0981E-1	3.6050E-1	5.1829E-1	8.2126E-1	7.2824E-1	5.8313E-1	1.650E-1	2.59E-1
502	1.4841E-1	4.3185E-1	2.9065E-1	3.2556E-1	3.7696E-1	5.3092E-1	8.3171E-1	7.3939E-1	5.9632E-1	1.630E-1	2.43E-1
503	1.4144E-1	4.5092E-1	3.0560E-1	3.4201E-1	3.9416E-1	5.4362E-1	8.4198E-1	7.5046E-1	6.0953E-1	1.610E-1	2.27E-1
504	1.3468E-1	4.7056E-1	3.2111E-1	3.5905E-1	4.1191E-1	5.5639E-1	8.5205E-1	7.6144E-1	6.2275E-1	1.590E-1	2.11E-1
505	1.2802E-1	4.9056E-1	3.3706E-1	3.7656E-1	4.3004E-1	5.6923E-1	8.6190E-1	7.7232E-1	6.3598E-1	1.570E-1	1.95E-1
506	1.2136E-1	5.1079E-1	3.5336E-1	3.9424E-1	4.4866E-1	5.8211E-1	8.7152E-1	7.8308E-1	6.4920E-1	1.550E-1	1.82E-1
507	1.1473E-1	5.3128E-1	3.7006E-1	4.1232E-1	4.6757E-1	5.9502E-1	8.8090E-1	7.9373E-1	6.6240E-1	1.530E-1	1.69E-1
508	1.0820E-1	5.5208E-1	3.8720E-1	4.3085E-1	4.8683E-1	6.0797E-1	8.9003E-1	8.0423E-1	6.7556E-1	1.510E-1	1.56E-1
509	1.0179E-1	5.7324E-1	4.0484E-1	4.4989E-1	5.0649E-1	6.2093E-1	8.9888E-1	8.1460E-1	6.8867E-1	1.490E-1	1.43E-1
510	9.5566E-2	5.9483E-1	4.2302E-1	4.6948E-1	5.2661E-1	6.3389E-1	9.0746E-1	8.2480E-1	7.0171E-1	1.470E-1	1.30E-1
511	8.9514E-2	6.1682E-1	4.4176E-1	4.8927E-1	5.4759E-1	6.4685E-1	9.1573E-1	8.3484E-1	7.1468E-1	1.456E-1	1.21E-1
512	8.3638E-2	6.3905E-1	4.6093E-1	5.0948E-1	5.6888E-1	6.5978E-1	9.2370E-1	8.4470E-1	7.2755E-1	1.442E-1	1.12E-1
513	7.7988E-2	6.6137E-1	4.8042E-1	5.2998E-1	5.9033E-1	6.7268E-1	9.3135E-1	8.5437E-1	7.4031E-1	1.428E-1	1.03E-1
514	7.2614E-2	6.8361E-1	5.0012E-1	5.5066E-1	6.1178E-1	6.8554E-1	9.3865E-1	8.6383E-1	7.5295E-1	1.414E-1	9.40E-2
515	6.7565E-2	7.0561E-1	5.1989E-1	5.7139E-1	6.3311E-1	6.9833E-1	9.4561E-1	8.7308E-1	7.6545E-1	1.400E-1	8.50E-2
516	6.2865E-2	7.2731E-1	5.3971E-1	5.9196E-1	6.5441E-1	7.1105E-1	9.5221E-1	8.8210E-1	7.7780E-1	1.386E-1	7.80E-2
517	5.8500E-2	7.4860E-1	5.5949E-1	6.1245E-1	6.7542E-1	7.2369E-1	9.5843E-1	8.9087E-1	7.8997E-1	1.372E-1	7.10E-2
518	5.4467E-2	7.6926E-1	5.7905E-1	6.3266E-1	6.9592E-1	7.3622E-1	9.6426E-1	8.9938E-1	8.0195E-1	1.358E-1	6.40E-2
519	5.0764E-2	7.8905E-1	5.9819E-1	6.5241E-1	7.1571E-1	7.4864E-1	9.6969E-1	9.0764E-1	8.1374E-1	1.344E-1	5.70E-2

Appendix A. Continued

Wavelength	Psychophysical Cone Fundamentals					Pigment Extinction Spectra				Lens	Macular
	S	M	L	M'	L'	L	M	L'	M'	Density	Density
520	4.7387E-2	8.0775E-1	6.1674E-1	6.7149E-1	7.3457E-1	7.6093E-1	9.7471E-1	9.1562E-1	8.2530E-1	1.330E-1	5.00E-2
521	4.4345E-2	8.2517E-1	6.3455E-1	6.8959E-1	7.5248E-1	7.7308E-1	9.7931E-1	9.2332E-1	8.3662E-1	1.317E-1	4.50E-2
522	4.1610E-2	8.4139E-1	6.5168E-1	7.0693E-1	7.6937E-1	7.8507E-1	9.8347E-1	9.3072E-1	8.4770E-1	1.304E-1	4.00E-2
523	3.9129E-2	8.5656E-1	6.6823E-1	7.2363E-1	7.8538E-1	7.9688E-1	9.8719E-1	9.3781E-1	8.5850E-1	1.291E-1	3.50E-2
524	3.6847E-2	8.7085E-1	6.8433E-1	7.3981E-1	8.0065E-1	8.0850E-1	9.9045E-1	9.4456E-1	8.6902E-1	1.278E-1	3.00E-2
525	3.4711E-2	8.8440E-1	7.0010E-1	7.5559E-1	8.1534E-1	8.1992E-1	9.9325E-1	9.5098E-1	8.7924E-1	1.265E-1	2.50E-2
526	3.2691E-2	8.9727E-1	7.1557E-1	7.7086E-1	8.2960E-1	8.3112E-1	9.9558E-1	9.5704E-1	8.8914E-1	1.252E-1	2.20E-2
527	3.0785E-2	9.0940E-1	7.3068E-1	7.8570E-1	8.4326E-1	8.4209E-1	9.9742E-1	9.6275E-1	8.9870E-1	1.239E-1	1.90E-2
528	2.8978E-2	9.2074E-1	7.4536E-1	8.0006E-1	8.5631E-1	8.5280E-1	9.9878E-1	9.6810E-1	9.0792E-1	1.226E-1	1.60E-2
529	2.7255E-2	9.3128E-1	7.5957E-1	8.1386E-1	8.6869E-1	8.6325E-1	9.9964E-1	9.7307E-1	9.1677E-1	1.213E-1	1.30E-2
530	2.5602E-2	9.4098E-1	7.7322E-1	8.2705E-1	8.8038E-1	8.7342E-1	1.0000E+0	9.7764E-1	9.2525E-1	1.200E-1	1.00E-2
531	2.4001E-2	9.4983E-1	7.8631E-1	8.3952E-1	8.9141E-1	8.8328E-1	9.9985E-1	9.8182E-1	9.3331E-1	1.187E-1	8.00E-3
532	2.2449E-2	9.5786E-1	7.9886E-1	8.5139E-1	9.0177E-1	8.9284E-1	9.9919E-1	9.8558E-1	9.4098E-1	1.174E-1	6.00E-3
533	2.0954E-2	9.6513E-1	8.1091E-1	8.6271E-1	9.1151E-1	9.0207E-1	9.9801E-1	9.8893E-1	9.4824E-1	1.161E-1	4.00E-3
534	1.9525E-2	9.7166E-1	8.2250E-1	8.7349E-1	9.2066E-1	9.1096E-1	9.9632E-1	9.9185E-1	9.5504E-1	1.148E-1	2.00E-3
535	1.8168E-2	9.7750E-1	8.3367E-1	8.8379E-1	9.2926E-1	9.1950E-1	9.9410E-1	9.9433E-1	9.6139E-1	1.135E-1	0
536	1.6884E-2	9.8267E-1	8.4443E-1	8.9352E-1	9.3732E-1	9.2767E-1	9.9136E-1	9.9638E-1	9.6730E-1	1.122E-1	0
537	1.5667E-2	9.8716E-1	8.5478E-1	9.0279E-1	9.4481E-1	9.3545E-1	9.8810E-1	9.9797E-1	9.7276E-1	1.109E-1	0
538	1.4517E-2	9.9098E-1	8.6471E-1	9.1158E-1	9.5176E-1	9.4284E-1	9.8431E-1	9.9911E-1	9.7770E-1	1.096E-1	0
539	1.3433E-2	9.9412E-1	8.7424E-1	9.1991E-1	9.5814E-1	9.4982E-1	9.8001E-1	9.9979E-1	9.8215E-1	1.083E-1	0
540	1.2414E-2	9.9658E-1	8.8336E-1	9.2781E-1	9.6395E-1	9.5637E-1	9.7518E-1	1.0000E+0	9.8615E-1	1.070E-1	0
541	1.1461E-2	9.9837E-1	8.9207E-1	9.3524E-1	9.6707E-1	9.6250E-1	9.7295E-1	9.9972E-1	9.8962E-1	1.056E-1	0
542	1.0570E-2	9.9951E-1	9.0040E-1	9.4222E-1	9.7149E-1	9.6819E-1	9.6751E-1	9.9898E-1	9.9254E-1	1.042E-1	0
543	9.7400E-3	1.0000E+0	9.0833E-1	9.4880E-1	9.7562E-1	9.7342E-1	9.6123E-1	9.9779E-1	9.9501E-1	1.028E-1	0
544	8.9691E-3	9.9986E-1	9.1589E-1	9.5495E-1	9.7939E-1	9.7820E-1	9.5416E-1	9.9607E-1	9.9696E-1	1.014E-1	0
545	8.2552E-3	9.9910E-1	9.2308E-1	9.6065E-1	9.8284E-1	9.8250E-1	9.4633E-1	9.9387E-1	9.9832E-1	1.000E-1	0
546	7.5968E-3	9.9772E-1	9.2988E-1	9.6596E-1	9.8600E-1	9.8633E-1	9.3777E-1	9.9122E-1	9.9923E-1	9.860E-2	0
547	6.9911E-3	9.9580E-1	9.3637E-1	9.7096E-1	9.8881E-1	9.8968E-1	9.2862E-1	9.8810E-1	9.9968E-1	9.720E-2	0
548	6.4344E-3	9.9318E-1	9.4244E-1	9.7572E-1	9.9122E-1	9.9254E-1	9.1867E-1	9.8441E-1	1.0000E+0	9.580E-2	0
549	5.9232E-3	9.9009E-1	9.4825E-1	9.7984E-1	9.9332E-1	9.9491E-1	9.0827E-1	9.8029E-1	9.9920E-1	9.440E-2	0
550	5.4539E-3	9.8652E-1	9.5381E-1	9.8356E-1	9.9509E-1	9.9678E-1	8.9741E-1	9.7573E-1	9.9771E-1	9.300E-2	0
551	5.0234E-3	9.8243E-1	9.5909E-1	9.8691E-1	9.9800E-1	9.9815E-1	8.8634E-1	9.7311E-1	9.9561E-1	9.170E-2	0
552	4.6298E-3	9.7784E-1	9.6410E-1	9.8994E-1	9.9946E-1	9.9902E-1	8.7482E-1	9.6848E-1	9.9301E-1	9.040E-2	0
553	4.2708E-3	9.7274E-1	9.6883E-1	9.9254E-1	1.0000E+0	9.9940E-1	8.6287E-1	9.6264E-1	9.8968E-1	8.910E-2	0
554	3.9441E-3	9.6714E-1	9.7328E-1	9.9429E-1	9.9990E-1	1.0000E+0	8.5050E-1	9.5597E-1	9.8574E-1	8.780E-2	0
555	3.6473E-3	9.6103E-1	9.7743E-1	9.9621E-1	9.9924E-1	9.9912E-1	8.3773E-1	9.4863E-1	9.8115E-1	8.650E-2	0
556	3.3786E-3	9.5440E-1	9.8129E-1	9.9769E-1	9.9802E-1	9.9772E-1	8.2456E-1	9.4062E-1	9.7590E-1	8.520E-2	0
557	3.1354E-3	9.4725E-1	9.8483E-1	9.9883E-1	9.9626E-1	9.9578E-1	8.1101E-1	9.3200E-1	9.7015E-1	8.390E-2	0
558	2.9152E-3	9.3955E-1	9.8803E-1	9.9957E-1	9.9391E-1	9.9327E-1	7.9708E-1	9.2272E-1	9.6384E-1	8.260E-2	0
559	2.7154E-3	9.3130E-1	9.9087E-1	9.9996E-1	9.9105E-1	9.9017E-1	7.8278E-1	9.1290E-1	9.5706E-1	8.130E-2	0
560	2.5331E-3	9.2249E-1	9.9332E-1	1.0000E+0	9.8774E-1	9.8645E-1	7.6810E-1	9.0265E-1	9.4982E-1	8.000E-2	0
561	2.3663E-3	9.1307E-1	9.9536E-1	9.9966E-1	9.8408E-1	9.8206E-1	7.5305E-1	8.9211E-1	9.4209E-1	7.870E-2	0
562	2.2139E-3	9.0312E-1	9.9700E-1	9.9896E-1	9.8005E-1	9.7710E-1	7.3769E-1	8.8126E-1	9.3393E-1	7.740E-2	0
563	2.0756E-3	8.9265E-1	9.9827E-1	9.9785E-1	9.7555E-1	9.7158E-1	7.2208E-1	8.6999E-1	9.2528E-1	7.610E-2	0
564	1.9509E-3	8.8168E-1	9.9919E-1	9.9625E-1	9.7060E-1	9.6556E-1	7.0625E-1	8.5835E-1	9.1605E-1	7.480E-2	0
565	1.8392E-3	8.7024E-1	9.9976E-1	9.9410E-1	9.6517E-1	9.5907E-1	6.9024E-1	8.4631E-1	9.0617E-1	7.350E-2	0
566	1.7394E-3	8.5835E-1	1.0000E+0	9.9156E-1	9.5925E-1	9.5213E-1	6.7409E-1	8.3390E-1	8.9589E-1	7.220E-2	0
567	1.6506E-3	8.4601E-1	9.9989E-1	9.8863E-1	9.5287E-1	9.4476E-1	6.5781E-1	8.2115E-1	8.8523E-1	7.090E-2	0
568	1.5722E-3	8.3322E-1	9.9942E-1	9.8532E-1	9.4596E-1	9.3694E-1	6.4141E-1	8.0800E-1	8.7424E-1	6.960E-2	0
569	1.5037E-3	8.2000E-1	9.9859E-1	9.8165E-1	9.3861E-1	9.2867E-1	6.2492E-1	7.9457E-1	8.6294E-1	6.830E-2	0
570	1.4446E-3	8.0635E-1	9.9737E-1	9.7760E-1	9.3067E-1	9.1997E-1	6.0835E-1	7.8072E-1	8.5136E-1	6.700E-2	0
571	1.3941E-3	7.9228E-1	9.9575E-1	9.7340E-1	9.2245E-1	9.1049E-1	5.9155E-1	7.6657E-1	8.3947E-1	6.560E-2	0
572	1.3513E-3	7.7781E-1	9.9376E-1	9.6879E-1	9.1368E-1	9.0062E-1	5.7474E-1	7.5208E-1	8.2729E-1	6.420E-2	0
573	1.3150E-3	7.6297E-1	9.9138E-1	9.6376E-1	9.0438E-1	8.9038E-1	5.5793E-1	7.3728E-1	8.1479E-1	6.280E-2	0
574	1.2844E-3	7.4778E-1	9.8864E-1	9.5843E-1	8.9465E-1	8.7980E-1	5.4116E-1	7.2231E-1	8.0218E-1	6.140E-2	0
575	1.2585E-3	7.3228E-1	9.8555E-1	9.5274E-1	8.8437E-1	8.6891E-1	5.2446E-1	7.0705E-1	7.8936E-1	6.000E-2	0
576	1.2369E-3	7.1649E-1	9.8210E-1	9.4666E-1	8.7373E-1	8.5774E-1	5.0786E-1	6.9172E-1	7.7632E-1	5.860E-2	0
577	1.2183E-3	7.0043E-1	9.7829E-1	9.4016E-1	8.6257E-1	8.4630E-1	4.9136E-1	6.7616E-1	7.6305E-1	5.720E-2	0
578	1.2008E-3	6.8411E-1	9.7411E-1	9.3332E-1	8.5107E-1	8.3457E-1	4.7499E-1	6.6055E-1	7.4965E-1	5.580E-2	0
579	1.1823E-3	6.6754E-1	9.6952E-1	9.2610E-1	8.3908E-1	8.2255E-1	4.5874E-1	6.4478E-1	7.3608E-1	5.440E-2	0

(continued overleaf)

Appendix A. Continued

Wavelength	Psychophysical Cone Fundamentals					Pigment Extinction Spectra				Lens Density	Macular Density
	S	M	L	M'	L'	L	M	L'	M'		
580	1.1608E-3	6.5073E-1	9.6453E-1	9.1856E-1	8.2673E-1	8.1024E-1	4.4263E-1	6.2897E-1	7.2244E-1	5.300E-2	0
581	1.1352E-3	6.3370E-1	9.5910E-1	9.1044E-1	8.1373E-1	7.9790E-1	4.2679E-1	6.1303E-1	7.0867E-1	5.170E-2	0
582	1.1060E-3	6.1648E-1	9.5328E-1	9.0207E-1	8.0025E-1	7.8531E-1	4.1111E-1	5.9696E-1	6.9491E-1	5.040E-2	0
583	1.0737E-3	5.9913E-1	9.4706E-1	8.9354E-1	7.8633E-1	7.7249E-1	3.9564E-1	5.8079E-1	6.8125E-1	4.910E-2	0
584	1.0388E-3	5.8168E-1	9.4048E-1	8.8561E-1	7.7206E-1	7.5949E-1	3.8038E-1	5.6463E-1	6.6851E-1	4.780E-2	0
585	1.0018E-3	5.6418E-1	9.3356E-1	8.7766E-1	7.5747E-1	7.4635E-1	3.6538E-1	5.4850E-1	6.5599E-1	4.650E-2	0
586	9.6191E-4	5.4665E-1	9.2630E-1	8.6944E-1	7.4258E-1	7.3309E-1	3.5065E-1	5.3242E-1	6.4343E-1	4.520E-2	0
587	9.2001E-4	5.2913E-1	9.1870E-1	8.6087E-1	7.2741E-1	7.1972E-1	3.3620E-1	5.1641E-1	6.3077E-1	4.390E-2	0
588	8.7909E-4	5.1166E-1	9.1081E-1	8.5192E-1	7.1198E-1	7.0628E-1	3.2205E-1	5.0050E-1	6.1799E-1	4.260E-2	0
589	8.4211E-4	4.9427E-1	9.0263E-1	8.4262E-1	6.9631E-1	6.9282E-1	3.0822E-1	4.8470E-1	6.0513E-1	4.130E-2	0
590	8.1208E-4	4.7699E-1	8.9420E-1	8.3291E-1	6.8041E-1	6.7935E-1	2.9472E-1	4.6901E-1	5.9212E-1	4.000E-2	0
591	7.9125E-4	4.5984E-1	8.8553E-1	8.2178E-1	6.6336E-1	6.6718E-1	2.8199E-1	4.5344E-1	5.7912E-1	3.930E-2	0
592	7.7743E-4	4.4288E-1	8.7663E-1	8.1036E-1	6.4620E-1	6.5498E-1	2.6956E-1	4.3804E-1	5.6607E-1	3.860E-2	0
593	7.6692E-4	4.2613E-1	8.6746E-1	7.9877E-1	6.2898E-1	6.4271E-1	2.5746E-1	4.2286E-1	5.5311E-1	3.790E-2	0
594	7.5602E-4	4.0964E-1	8.5799E-1	7.8713E-1	6.1166E-1	6.3035E-1	2.4571E-1	4.0784E-1	5.4033E-1	3.720E-2	0
595	7.4104E-4	3.9346E-1	8.4818E-1	7.7526E-1	5.9426E-1	6.1788E-1	2.3433E-1	3.9302E-1	5.2758E-1	3.650E-2	0
596	7.1999E-4	3.7762E-1	8.3804E-1	7.6319E-1	5.7681E-1	6.0529E-1	2.2333E-1	3.7840E-1	5.1488E-1	3.580E-2	0
597	6.9455E-4	3.6214E-1	8.2757E-1	7.5081E-1	5.5937E-1	5.9262E-1	2.1271E-1	3.6402E-1	5.0214E-1	3.510E-2	0
598	6.6654E-4	3.4699E-1	8.1681E-1	7.3815E-1	5.4194E-1	5.7989E-1	2.0243E-1	3.4988E-1	4.8939E-1	3.440E-2	0
599	6.3773E-4	3.3216E-1	8.0581E-1	7.2521E-1	5.2458E-1	5.6717E-1	1.9250E-1	3.3602E-1	4.7663E-1	3.370E-2	0
600	6.1000E-4	3.1763E-1	7.9460E-1	7.1198E-1	5.0731E-1	5.5448E-1	1.8288E-1	3.2244E-1	4.6387E-1	3.300E-2	0
601	5.8433E-4	3.0340E-1	7.8321E-1	6.9840E-1	4.9000E-1	5.4200E-1	1.7360E-1	3.0912E-1	4.5118E-1	3.240E-2	0
602	5.5972E-4	2.8949E-1	7.7162E-1	6.8465E-1	4.7300E-1	5.2957E-1	1.6464E-1	2.9621E-1	4.3857E-1	3.180E-2	0
603	5.3481E-4	2.7595E-1	7.5982E-1	6.7072E-1	4.5648E-1	5.1715E-1	1.5601E-1	2.8383E-1	4.2604E-1	3.120E-2	0
604	5.0830E-4	2.6282E-1	7.4776E-1	6.5659E-1	4.4032E-1	5.0474E-1	1.4771E-1	2.7186E-1	4.1357E-1	3.060E-2	0
605	4.7883E-4	2.5012E-1	7.3544E-1	6.4235E-1	4.2434E-1	4.9230E-1	1.3977E-1	2.6018E-1	4.0123E-1	3.000E-2	0
606	4.4540E-4	2.3787E-1	7.2283E-1	6.2798E-1	4.0857E-1	4.7984E-1	1.3218E-1	2.4880E-1	3.8900E-1	2.940E-2	0
607	4.0952E-4	2.2608E-1	7.0996E-1	6.1349E-1	3.9312E-1	4.6738E-1	1.2494E-1	2.3780E-1	3.7689E-1	2.880E-2	0
608	3.7369E-4	2.1473E-1	6.9689E-1	5.9888E-1	3.7794E-1	4.5496E-1	1.1803E-1	2.2711E-1	3.6490E-1	2.820E-2	0
609	3.4038E-4	2.0381E-1	6.8366E-1	5.8417E-1	3.6310E-1	4.4262E-1	1.1144E-1	2.1678E-1	3.5303E-1	2.760E-2	0
610	3.1212E-4	1.9331E-1	6.7030E-1	5.6932E-1	3.4859E-1	4.3040E-1	1.0515E-1	2.0679E-1	3.4126E-1	2.700E-2	0
611	2.9021E-4	1.8323E-1	6.5684E-1	5.5443E-1	3.3443E-1	4.1818E-1	9.9141E-2	1.9710E-1	3.2957E-1	2.630E-2	0
612	2.7345E-4	1.7357E-1	6.4327E-1	5.3930E-1	3.2056E-1	4.0609E-1	9.3427E-2	1.8772E-1	3.1791E-1	2.560E-2	0
613	2.6045E-4	1.6432E-1	6.2958E-1	5.2391E-1	3.0699E-1	3.9411E-1	8.7997E-2	1.7865E-1	3.0627E-1	2.490E-2	0
614	2.4987E-4	1.5547E-1	6.1577E-1	5.0830E-1	2.9374E-1	3.8225E-1	8.2841E-2	1.6988E-1	2.9468E-1	2.420E-2	0
615	2.4036E-4	1.4701E-1	6.0183E-1	4.9254E-1	2.8079E-1	3.7049E-1	7.7949E-2	1.6140E-1	2.8318E-1	2.350E-2	0
616	2.3168E-4	1.3894E-1	5.8778E-1	4.7673E-1	2.6818E-1	3.5885E-1	7.3314E-2	1.5323E-1	2.7185E-1	2.280E-2	0
617	2.2390E-4	1.3124E-1	5.7362E-1	4.6093E-1	2.5596E-1	3.4733E-1	6.8924E-2	1.4539E-1	2.6070E-1	2.210E-2	0
618	2.1624E-4	1.2389E-1	5.5931E-1	4.4520E-1	2.4410E-1	3.3589E-1	6.4761E-2	1.3785E-1	2.4978E-1	2.140E-2	0
619	2.0793E-4	1.1687E-1	5.4481E-1	4.2960E-1	2.3265E-1	3.2451E-1	6.0810E-2	1.3064E-1	2.3912E-1	2.070E-2	0
620	1.9817E-4	1.1015E-1	5.3006E-1	4.1418E-1	2.2165E-1	3.1314E-1	5.7055E-2	1.2378E-1	2.2873E-1	2.000E-2	0
621	1.8627E-4	1.0371E-1	5.1507E-1	3.9901E-1	2.1100E-1	3.0180E-1	5.3483E-2	1.1718E-1	2.1866E-1	1.930E-2	0
622	1.7271E-4	9.7561E-2	4.9988E-1	3.8430E-1	2.0070E-1	2.9051E-1	5.0091E-2	1.1087E-1	2.0903E-1	1.860E-2	0
623	1.5849E-4	9.1694E-2	4.8458E-1	3.7011E-1	1.9088E-1	2.7934E-1	4.6875E-2	1.0489E-1	1.9984E-1	1.790E-2	0
624	1.4462E-4	8.6112E-2	4.6925E-1	3.5634E-1	1.8134E-1	2.6833E-1	4.3834E-2	9.9133E-2	1.9104E-1	1.720E-2	0
625	1.3211E-4	8.0815E-2	4.5397E-1	3.4296E-1	1.7211E-1	2.5752E-1	4.0965E-2	9.3610E-2	1.8258E-1	1.650E-2	0
626	1.2138E-4	7.5796E-2	4.3876E-1	3.2998E-1	1.6339E-1	2.4694E-1	3.8262E-2	8.8428E-2	1.7447E-1	1.580E-2	0
627	1.1206E-4	7.1045E-2	4.2366E-1	3.1723E-1	1.5498E-1	2.3659E-1	3.5718E-2	8.3463E-2	1.6660E-1	1.510E-2	0
628	1.0393E-4	6.6554E-2	4.0876E-1	3.0469E-1	1.4686E-1	2.2652E-1	3.3325E-2	7.8711E-2	1.5896E-1	1.440E-2	0
629	9.6756E-5	6.2319E-2	3.9415E-1	2.9242E-1	1.3917E-1	2.1679E-1	3.1081E-2	7.4236E-2	1.5157E-1	1.370E-2	0
630	9.0315E-5	5.8332E-2	3.7994E-1	2.8046E-1	1.3182E-1	2.0743E-1	2.8978E-2	6.9990E-2	1.4444E-1	1.300E-2	0
631	8.4598E-5	5.4588E-2	3.6618E-1	2.6866E-1	1.2472E-1	1.9854E-1	2.7020E-2	6.5931E-2	1.3752E-1	1.240E-2	0
632	7.9649E-5	5.1076E-2	3.5285E-1	2.5708E-1	1.1793E-1	1.9002E-1	2.5190E-2	6.2079E-2	1.3081E-1	1.180E-2	0
633	7.5305E-5	4.7777E-2	3.3988E-1	2.4570E-1	1.1146E-1	1.8183E-1	2.3480E-2	5.8422E-2	1.2428E-1	1.120E-2	0
634	7.1413E-5	4.4676E-2	3.2723E-1	2.3463E-1	1.0524E-1	1.7392E-1	2.1879E-2	5.4933E-2	1.1800E-1	1.060E-2	0
635	6.7831E-5	4.1757E-2	3.1482E-1	2.2382E-1	9.9261E-2	1.6626E-1	2.0379E-2	5.1602E-2	1.1192E-1	1.000E-2	0
636	6.4465E-5	3.9007E-2	3.0264E-1	2.1328E-1	9.3564E-2	1.5883E-1	1.8971E-2	4.8445E-2	1.0605E-1	9.400E-3	0
637	6.1290E-5	3.6421E-2	2.9072E-1	2.0303E-1	8.8120E-2	1.5163E-1	1.7653E-2	4.5445E-2	1.0040E-1	8.800E-3	0
638	5.8264E-5	3.3990E-2	2.7904E-1	1.9312E-1	8.2935E-2	1.4466E-1	1.6419E-2	4.2603E-2	9.4981E-2	8.200E-3	0
639	5.5334E-5	3.1704E-2	2.6761E-1	1.8354E-1	7.8011E-2	1.3790E-1	1.5264E-2	3.9919E-2	8.9795E-2	7.600E-3	0

Appendix A. Continued

Wavelength	Psychophysical Cone Fundamentals					Pigment Extinction Spectra				Lens Density	Macular Density
	S	M	L	M'	L'	L	M	L'	M'		
640	5.2457E-5	2.9558E-2	2.5642E-1	1.7427E-1	7.3352E-2	1.3136E-1	1.4183E-2	3.7392E-2	8.4818E-2	7.000E-3	0
641	4.9588E-5	2.7539E-2	2.4546E-1	1.6536E-1	6.8923E-2	1.2498E-1	1.3168E-2	3.4995E-2	8.0051E-2	6.300E-3	0
642	4.6724E-5	2.5643E-2	2.3474E-1	1.5691E-1	6.4739E-2	1.1881E-1	1.2219E-2	3.2740E-2	7.5564E-2	5.600E-3	0
643	4.3865E-5	2.3868E-2	2.2427E-1	1.4897E-1	6.0797E-2	1.1285E-1	1.1333E-2	3.0628E-2	7.1377E-2	4.900E-3	0
644	4.1011E-5	2.2209E-2	2.1407E-1	1.4136E-1	5.7089E-2	1.0710E-1	1.0509E-2	2.8649E-2	6.7394E-2	4.200E-3	0
645	3.8166E-5	2.0664E-2	2.0415E-1	1.3403E-1	5.3583E-2	1.0156E-1	9.7448E-3	2.6788E-2	6.3588E-2	3.500E-3	0
646	3.5292E-5	1.9229E-2	1.9452E-1	1.2696E-1	5.0266E-2	9.6229E-2	9.0372E-3	2.5035E-2	5.9943E-2	2.800E-3	0
647	3.2427E-5	1.7896E-2	1.8518E-1	1.2017E-1	4.7179E-2	9.1107E-2	8.3822E-3	2.3411E-2	5.6471E-2	2.100E-3	0
648	2.9693E-5	1.6657E-2	1.7614E-1	1.1363E-1	4.4273E-2	8.6195E-2	7.7757E-3	2.1888E-2	5.3146E-2	1.400E-3	0
649	2.7204E-5	1.5504E-2	1.6742E-1	1.0734E-1	4.1514E-2	8.1494E-2	7.2135E-3	2.0449E-2	4.9974E-2	7.000E-4	0
650	2.5084E-5	1.4430E-2	1.5903E-1	1.0130E-1	3.8896E-2	7.7008E-2	6.6914E-3	1.9090E-2	4.6952E-2	0	0
651	2.3804E-5	1.3429E-2	1.5097E-1	9.5352E-2	3.6365E-2	7.2859E-2	6.2164E-3	1.7813E-2	4.4067E-2	0	0
652	2.2579E-5	1.2496E-2	1.4325E-1	8.9670E-2	3.4009E-2	6.8902E-2	5.7747E-3	1.6627E-2	4.1326E-2	0	0
653	2.1399E-5	1.1627E-2	1.3584E-1	8.4238E-2	3.1788E-2	6.5123E-2	5.3641E-3	1.5511E-2	3.8716E-2	0	0
654	2.0270E-5	1.0817E-2	1.2871E-1	7.9044E-2	2.9689E-2	6.1512E-2	4.9823E-3	1.4459E-2	3.6232E-2	0	0
655	1.9184E-5	1.0063E-2	1.2186E-1	7.4086E-2	2.7701E-2	5.8055E-2	4.6272E-3	1.3466E-2	3.3871E-2	0	0
656	1.8140E-5	9.3584E-3	1.1526E-1	6.9384E-2	2.5838E-2	5.4746E-2	4.2963E-3	1.2537E-2	3.1641E-2	0	0
657	1.7137E-5	8.7015E-3	1.0892E-1	6.4920E-2	2.4092E-2	5.1583E-2	3.9882E-3	1.1669E-2	2.9532E-2	0	0
658	1.6174E-5	8.0894E-3	1.0284E-1	6.0705E-2	2.2461E-2	4.8562E-2	3.7017E-3	1.0859E-2	2.7547E-2	0	0
659	1.5252E-5	7.5198E-3	9.7011E-2	5.6730E-2	2.0934E-2	4.5678E-2	3.4355E-3	1.0103E-2	2.5682E-2	0	0
660	1.4370E-5	6.9904E-3	9.1421E-2	5.2996E-2	1.9506E-2	4.2927E-2	3.1885E-3	9.3972E-3	2.3936E-2	0	0
661	1.3526E-5	6.4987E-3	8.6069E-2	4.9510E-2	1.8182E-2	4.0304E-2	2.9595E-3	8.7441E-3	2.2311E-2	0	0
662	1.2719E-5	6.0419E-3	8.0950E-2	4.6275E-2	1.6954E-2	3.7807E-2	2.7472E-3	8.1394E-3	2.0808E-2	0	0
663	1.1948E-5	5.6168E-3	7.6062E-2	4.3279E-2	1.5805E-2	3.5432E-2	2.5499E-3	7.5752E-3	1.9419E-2	0	0
664	1.1215E-5	5.2204E-3	7.1404E-2	4.0515E-2	1.4731E-2	3.3177E-2	2.3662E-3	7.0483E-3	1.8140E-2	0	0
665	1.0516E-5	4.8495E-3	6.6972E-2	3.7978E-2	1.3738E-2	3.1041E-2	2.1946E-3	6.5622E-3	1.6970E-2	0	0
666	9.8532E-6	4.5012E-3	6.2759E-2	3.5620E-2	1.2824E-2	2.9018E-2	2.0338E-3	6.1155E-3	1.5884E-2	0	0
667	9.2246E-6	4.1748E-3	5.8764E-2	3.3430E-2	1.1975E-2	2.7106E-2	1.8834E-3	5.7010E-3	1.4879E-2	0	0
668	8.6312E-6	3.8705E-3	5.4995E-2	3.1391E-2	1.1180E-2	2.5309E-2	1.7434E-3	5.3141E-3	1.3944E-2	0	0
669	8.0756E-6	3.5888E-3	5.1460E-2	2.9476E-2	1.0435E-2	2.3628E-2	1.6141E-3	4.9521E-3	1.3069E-2	0	0
670	7.5565E-6	3.3299E-3	4.8166E-2	2.7653E-2	9.7371E-3	2.2067E-2	1.4953E-3	4.6133E-3	1.2237E-2	0	0
671	7.0776E-6	3.0932E-3	4.5115E-2	2.5892E-2	9.0823E-3	2.0625E-2	1.3869E-3	4.2962E-3	1.1437E-2	0	0
672	6.6334E-6	2.8764E-3	4.2289E-2	2.4174E-2	8.4682E-3	1.9292E-2	1.2878E-3	3.9993E-3	1.0658E-2	0	0
673	6.2219E-6	2.6776E-3	3.9669E-2	2.2507E-2	7.8998E-3	1.8060E-2	1.1969E-3	3.7250E-3	9.9050E-3	0	0
674	5.8393E-6	2.4947E-3	3.7237E-2	2.0908E-2	7.3706E-3	1.6919E-2	1.1135E-3	3.4700E-3	9.1848E-3	0	0
675	5.4846E-6	2.3257E-3	3.4975E-2	1.9395E-2	6.8759E-3	1.5860E-2	1.0365E-3	3.2320E-3	8.5047E-3	0	0
676	5.1544E-6	2.1693E-3	3.2876E-2	1.7983E-2	6.4138E-3	1.4879E-2	9.6534E-4	3.0101E-3	7.8719E-3	0	0
677	4.8477E-6	2.0247E-3	3.0925E-2	1.6668E-2	5.9821E-3	1.3970E-2	8.9961E-4	2.8032E-3	7.2835E-3	0	0
678	4.5602E-6	1.8898E-3	2.9094E-2	1.5443E-2	5.5787E-3	1.3118E-2	8.3842E-4	2.6101E-3	6.7362E-3	0	0
679	4.2867E-6	1.7627E-3	2.7351E-2	1.4303E-2	5.2010E-3	1.2309E-2	7.8086E-4	2.4297E-3	6.2285E-3	0	0
680	4.0220E-6	1.6414E-3	2.5667E-2	1.3247E-2	4.8484E-3	1.1530E-2	7.2607E-4	2.2615E-3	5.7588E-3	0	0
681	3.7634E-6	1.5243E-3	2.4019E-2	1.2272E-2	4.5174E-3	1.0770E-2	6.7327E-4	2.1039E-3	5.3261E-3	0	0
682	3.5116E-6	1.4117E-3	2.2414E-2	1.1376E-2	4.2057E-3	1.0033E-2	6.2257E-4	1.9557E-3	4.9291E-3	0	0
683	3.2693E-6	1.3045E-3	2.0869E-2	1.0555E-2	3.9131E-3	9.3244E-3	5.7447E-4	1.8169E-3	4.5658E-3	0	0
684	3.0384E-6	1.2039E-3	1.9400E-2	9.8031E-3	3.6401E-3	8.6525E-3	5.2939E-4	1.6876E-3	4.2338E-3	0	0
685	2.8222E-6	1.1111E-3	1.8022E-2	9.1183E-3	3.3880E-3	8.0237E-3	4.8784E-4	1.5684E-3	3.9318E-3	0	0
686	2.6209E-6	1.0261E-3	1.6737E-2	8.4922E-3	3.1555E-3	7.4391E-3	4.4985E-4	1.4586E-3	3.6560E-3	0	0
687	2.4330E-6	9.4805E-4	1.5538E-2	7.9205E-3	2.9417E-3	6.8942E-3	4.1504E-4	1.3577E-3	3.4045E-3	0	0
688	2.2580E-6	8.7645E-4	1.4421E-2	7.3971E-3	2.7451E-3	6.3877E-3	3.8313E-4	1.2651E-3	3.1746E-3	0	0
689	2.0953E-6	8.1071E-4	1.3383E-2	6.9138E-3	2.5647E-3	5.9181E-3	3.5388E-4	1.1802E-3	2.9626E-3	0	0
690	1.9449E-6	7.5025E-4	1.2422E-2	6.4630E-3	2.3980E-3	5.4840E-3	3.2701E-4	1.1019E-3	2.7651E-3	0	0
691	1.8060E-6	6.9474E-4	1.1536E-2	6.0382E-3	2.2433E-3	5.0847E-3	3.0237E-4	1.0293E-3	2.5794E-3	0	0
692	1.6786E-6	6.4400E-4	1.0722E-2	5.6367E-3	2.0995E-3	4.7184E-3	2.7988E-4	9.6188E-4	2.4042E-3	0	0
693	1.5617E-6	5.9768E-4	9.9758E-3	5.2586E-3	1.9656E-3	4.3829E-3	2.5937E-4	8.9923E-4	2.2396E-3	0	0
694	1.4544E-6	5.5540E-4	9.2910E-3	4.9044E-3	1.8402E-3	4.0755E-3	2.4068E-4	8.4063E-4	2.0856E-3	0	0
695	1.3559E-6	5.1682E-4	8.6627E-3	4.5743E-3	1.7217E-3	3.7940E-3	2.2363E-4	7.8532E-4	1.9423E-3	0	0
696	1.2660E-6	4.8167E-4	8.0881E-3	4.2675E-3	1.6084E-3	3.5368E-3	2.0813E-4	7.3259E-4	1.8093E-3	0	0
697	1.1838E-6	4.4962E-4	7.5629E-3	3.9818E-3	1.4993E-3	3.3021E-3	1.9399E-4	6.8188E-4	1.6856E-3	0	0
698	1.1081E-6	4.2027E-4	7.0798E-3	3.7153E-3	1.3940E-3	3.0864E-3	1.8107E-4	6.3309E-4	1.5705E-3	0	0
699	1.0380E-6	3.9325E-4	6.6314E-3	3.4664E-3	1.2934E-3	2.8865E-3	1.6919E-4	5.8655E-4	1.4631E-3	0	0
700	9.7208E-7	3.6828E-4	6.2104E-3	3.2334E-3	1.1983E-3	2.6992E-3	1.5822E-4	5.4266E-4	1.3627E-3	0	0

REFERENCES AND NOTES

- V. C. Smith and J. Pokorny, "Spectral sensitivity of the foveal cone photopigments between 400 and 500 nm," *Vision Res.* **15**, 161-171 (1975).
- D. I. A. MacLeod and R. M. Boynton, "Chromaticity diagram showing cone excitation by stimuli of equal luminance," *J. Opt. Soc. Am.* **69**, 1183-1186 (1979).
- A. M. Derrington, J. Krauskopf, and P. Lennie, "Chromatic mechanisms in lateral geniculate nucleus of macaque," *J. Physiol.* **357**, 241-265 (1984).
- J. v. Kries, "Ueber Farbensysteme," *Z. Psychol. Physiol. Sinnesorg.* **13**, 241-324 (1897).
- L. M. Hurvich, "Color vision deficiencies," in *Handbook of Sensory Physiology*, D. Jameson and L. M. Hurvich, eds. (Springer-Verlag, Berlin, 1972), Vol. 7.
- J. Pokorny, V. C. Smith, G. Verriest, and A. J. L. G. Pinckers, *Congenital and Acquired Color Vision Defects* (Grune & Stratton, New York, 1979).
- With larger fields, dichromats make matches similar to those of anomalous trichromats: A. L. Nagy, "Large-field substitution Rayleigh matches of dichromats," *J. Opt. Soc. Am.* **70**, 778-784 (1980); M. Breton and W. Cowan, "Deuteranomalous color matching in the deuteranopic eye," *J. Opt. Soc. Am.* **71**, 1220-1223 (1981).
- J. Nathans, D. Thomas, and D. S. Hogness, "Molecular genetics of human color vision: the genes encoding blue, green and red pigments," *Science* **232**, 193-202 (1986).
- J. Nathans, T. P. Piantanida, R. L. Eddy, T. B. Shows, and D. S. Hogness, "Molecular genetics of inherited variation in human color vision," *Science* **232**, 203-210 (1986).
- J. Pokorny and V. C. Smith, "Evaluation of single pigment shift model of anomalous trichromacy," *J. Opt. Soc. Am.* **67**, 1196-1209 (1977).
- J. Pokorny, V. C. Smith, and I. Katz, "Derivation of the photopigment absorption spectra in anomalous trichromats," *J. Opt. Soc. Am.* **63**, 232-237 (1973).
- J. Pokorny, J. D. Moreland, and V. C. Smith, "Photopigments in anomalous trichromats," *J. Opt. Soc. Am.* **65**, 1522-1524 (1975).
- J. J. Vos and P. L. Walraven, "On the derivation of the foveal receptor primaries," *Vision Res.* **11**, 799-818 (1971).
- I. Schmidt, "Some problems related to testing color vision with the Nagel anomaloscope," *J. Opt. Soc. Am.* **45**, 514-522 (1955).
- A. König and C. Dieterici, "Die Grundempfindungen und ihre Intensitäts-Vertheilung im Spectrum," *Sitz. Akad. Wiss. (Berlin)* (1886), pp. 805-829.
- A. König and C. Dieterici, "Die Grundempfindungen in normalen und anomalen Farben Systemen und ihre Intensitäts-Vertheilung im Spectrum," *Z. Psychol. Physiol. Sinnesorg.* **4**, 241-347 (1893).
- G. Wald, P. K. Brown, and P. H. Smith, "Iodopsin," *J. Gen. Physiol.* **38**, 623-681 (1955).
- D. A. Baylor, B. J. Nunn, and J. L. Schnapf, "Spectral sensitivity of cone of the monkey *Macaca fascicularis*," *J. Physiol.* **390**, 145-160 (1987).
- J. L. Schnapf, T. W. Kraft, B. J. Nunn, and D. A. Baylor, "Spectral sensitivity of primate photoreceptors," *Vis. Neurosci.* **1**, 255-261 (1988).
- D. B. Judd, "Colorimetry and artificial daylight," Technical Committee No. 7 Report of Secretariat, U.S. Commission, International Commission on Illumination, Twelfth Session (CIE, Paris, 1951).
- H. J. A. Dartnall, J. K. Bowmaker, and J. D. Mollon, "Human visual pigments: microspectrophotometric results from the eyes of seven persons," *Proc. R. Soc. London Ser. B* **220**, 115-130 (1983).
- J. Neitz and G. H. Jacobs, "Polymorphism in normal human color vision and its mechanism," *Vision Res.* **30**, 621-636 (1990).
- D. T. Lindsey, J. Winderickx, E. Sanocki, D. Teller, and A. G. Motulsky, "Individual differences in Rayleigh matches are related to differences in L cone pigment structure," in *Advances in Color Vision*, Vol. 4 of 1992 OSA Technical Digest Series (Optical Society of America, Washington, D.C., 1992).
- J. Neitz and M. Neitz, "The molecular genetic basis of polymorphism in normal color vision," in *Advances in Color Vision*, Vol. 4 of 1992 OSA Technical Digest Series (Optical Society of America, Washington, D.C., 1992).
- V. C. Smith, J. Pokorny, and K. R. Diddie, "Color matching and Stiles-Crawford effect in central serous choroidopathy," *Mod. Probl. Ophthalmol.* **19**, 284-295 (1978).
- V. C. Smith and J. Pokorny, "Spectral sensitivity of color-blind observers and the human cone photopigments," *Vision Res.* **12**, 2059-2071 (1972).
- T. G. Ebry and B. Honig, "New wavelength dependent visual pigment nomograms," *Vision Res.* **17**, 147-151 (1977).
- H. B. Barlow, "What causes trichromacy? A theoretical analysis using comb-filtered spectra," *Vision Res.* **22**, 635-643 (1982).
- R. J. W. Mansfield, "Primate photopigments and cone mechanisms," in *The Visual System*, A. Fein and J. S. Levine, eds. (Liss, New York, 1985).
- J. J. Vos, "Colorimetric and photometric properties of a 2° fundamental observer," *Color Res. Appl.* **3**, 125-128 (1978).
- R. W. Rodieck, *The Vertebrate Retina* (Freeman, San Francisco, Calif. 1973).
- J. Pokorny, V. C. Smith, and M. Lutze, "Aging of the human lens," *Appl. Opt.* **26**, 1437-1440 (1987).
- G. Wyszecki and W. S. Stiles, *Color Science—Concepts and Methods, Quantitative Data and Formulae* (Wiley, New York, 1982).
- M. E. Breton and R. W. Massof, "Short-wave irregularities in cone fundamentals," *J. Opt. Soc. Am. A* **2**, P23 (1985).
- W. D. Wright, "A re-determination of the trichromatic coefficients of the spectral colours," *Trans. Opt. Soc.* **30**, 141-164 (1929).
- J. Guild, "The colorimetric properties of the spectrum," *Philos. Trans. R. Soc. London Ser. A* **230**, 149-187 (1931).
- T. Smith and J. Guild, "The C.I.E. colorimetric standards and their use," *Trans. Opt. Soc.* **33**, 73-134 (1932).
- J. Pokorny, V. C. Smith, and S. J. Starr, "Variability of color mixture data—II. The effect of viewing field size on the unit coordinates," *Vision Res.* **16**, 1095-1098 (1976).
- J. L. Schnapf, T. W. Kraft, and D. A. Baylor, "Spectral sensitivity of human cone photoreceptors," *Nature (London)* **325**, 439-441 (1987).
- G. H. Jacobs, "Variations in colour vision in non-human primates," in *Inherited and Acquired Colour Vision Deficiencies*, D. H. Foster, ed. (CRC, Boca Raton, Fla., 1991).
- W. D. Wright, *Researches on Normal and Defective Colour Vision* (Kimpton, London, 1946).
- J. E. Thornton and E. N. J. Pugh, "Red/green color opponency at detection threshold," *Science* **219**, 191-193 (1983).
- L. M. Hurvich and D. Jameson, "Does anomalous color vision imply color weakness?" *Psychon. Sci.* **1**, 11-12 (1964).
- The authors will provide Appendix A as a text file on floppy disk in either MS-DOS or Macintosh operating system format.